



Spatial hybrid/parallel force control of a hexapod machine tool using structure-integrated force sensors and a commercial numerical control[☆]

C. Friedrich ^{*}, F. Schlüter, S. Ihlenfeldt

*Business Unit Cognitive Production, Fraunhofer Institute for Machine Tools and Forming Technology, Pforzheimer Straße 7a, 01189 Dresden, Germany
Chair of Machine Tool Development and Adaptive Controls, Institute of Mechatronic Engineering, TU Dresden, Helmholtzstrasse 7a, 01069 Dresden, Germany*

ARTICLE INFO

Keywords:

Machine tools
Force measurement
Force control
Robotics
Hexapod
Parallel kinematic machines
Sensor integration

ABSTRACT

Structure-integrated force measurement in hexapod structures or kinematics offers great potential for spatial process force control in six degrees of freedom. Although force control has been studied for many years, research questions remain unanswered, especially when regarding parallel kinematic machine tools with numerical control and integrated sensors. This contribution summarizes the technology of structure-integrated force sensing in hexapod machine tools and develops two approaches to use the measured signals for direct hybrid/parallel force control. For different use-cases, such as teach-in or synchronous force/position control with variable task frame, different approaches of set-point specification and injection of manipulated values are studied from a practical point of view. As a result of the work, the feasibility of the force control with structure-integrated sensors on a commercial CNC can be confirmed through appropriate experiments. Furthermore, the realized G-Code integration represents a practical solution for programming force-controlled machine tools in an easy and concise way from the NC programme.

1. Introduction and state of the art

Force measurement is essential for many manufacturing applications in production industry, such as milling, grinding, or thermo-smoothing, for the purpose of process monitoring and diagnosis, quality assurance, or tool condition monitoring. One step further, force control does not only allow to observe but also to react and, as a consequence, increase quality, tool life times, and productivity. Both, force measurement and control, require the integration of force sensors and, nowadays, the measurement of spatial forces and moments in 6 degrees of freedom (DoF) is requested, in particular.

A new sensing approach includes six 1 DoF force sensors into hexapod struts of hexapod kinematics or rigid hexapod-structures, such as clamping tables or end-effectors, to measure forces and moments at the tool centre point (TCP), whereby the measured forces are transformed to Cartesian by a control-integrated measurement model [1–5].

This paper presents the spatial hybrid/parallel force control of a hexapod machine tool that bases on the new structure-integrated force sensor system and a commercial numeric control system. Hereby, the feasibility of force control of a hexapod using structure-integrated force sensors is proven, and, further, new aspects regarding force control with numeric control in practice are presented.

1.1. Structure-integrated force measurement for hexapods

There are numerous ways to measure spatial forces and moments in robots and machine tools, which can be grouped in the application of commercial 6 DoF force/torque transducers (FT sensors) to the end-effector, the sensing within joints or structure parts, and the acquisition of drive currents. Sensors applied to the end-effector are highly accurate but lead to a reduction of usable work space, cause restrictions to spindle mounting or the machine's ruggedness (e.g. regarding cutting fluids), and also entail high financial costs. On the other hand, forces and moments that are indirectly obtained from drive currents are very limited in accuracy because of interfering non-linear and stochastic influences in the drive train, such as friction, stick-slip effects, or elastic deformations [2,5].

For this reasons, machine-integrated force measurement solutions have been studied since the beginning of force measurement [6]. The application of strain-gauges to machine components with specific design has been evaluated for end-effectors [7,8], spindles [9–11], clamping systems [12–14], grippers [15], a Z-slide [16], or even the workpiece [17]. However, these individual solutions are cost-intensive and do not provide a spatial measurement in 6 DoF so far [2,5].

[☆] This paper was recommended for publication by Associate Editor Chris Manzie.

* Corresponding author at: Business Unit Cognitive Production, Fraunhofer Institute for Machine Tools and Forming Technology, Pforzheimer Straße 7a, 01189 Dresden, Germany.

E-mail address: Christian.Friedrich@iwu.fraunhofer.de (C. Friedrich).

URL: <https://www.iwu.fraunhofer.de> (C. Friedrich).

Integrated torque sensors in joints are mainly applicable for industrial robots, where they are used for spatial force measurement and control at the TCP, e.g. for collaborative light-weight robots [18,19], or the identification of dynamic parameters [20,21]. However, joint torque measurement requires high mechanical and modelling efforts with regard to friction and stick-slip effects and is not advantageous for the desired application in parallel structures and kinematics, where mainly longitudinal forces appear.

Within Stewart or hexapod structures, forces can be measured using longitudinal sensors without friction or stick-slip effects. This principle is used to develop Stewart platform based force sensors, which has been studied in many works [22–26]. The most promising contributions present a multicomponent calibration system [27,28], a sensor for heavy duty applications [29–31], miniaturized sensors, e.g. for surgery, [32,33], and a measuring system for industrial applications [34]. However, all of these measuring devices have been designed as rigid sensor systems with static calibration, where no kinematic or dynamic influences need to be respected within a measurement model, due to the absence of motion.

In contrast to this, measurement models are mandatory for the measuring systems and use cases presented in this contribution (Section 2). Real-time capable measurement models that run within the numeric control system are essential for accurate measurement and they have been developed and validated in [1,2,4,5]. On this basis, [35] realized structure-integrated force measurement while replacing the measurement model by a linear neural network. As further shown in [2,5], accurate and precise spatial force measurements as well as competitive characteristics in resolution, range, and overload can be realized in the entire workspace, when compared to a commercial FT sensor. Also, the resulting stiffness at the TCP after sensor integration is evaluated to be comparable to a commercial FT sensor, as presented in [3,36]. Finally, model parameter identification procedures are studied in [4], since some of the model parameters, such as mass, centre of gravity and inertia, can change during machine usage, for example by a workpiece or tool change. Altogether, structure-integrated force measurement has many benefits for hexapod kinematics, as it fulfills accuracy and stiffness requirements, and is simple to parametrize.

In future, integrated sensors could already be supplied by the machine manufacturer and make force measurement and control an easy-to-use machine-integrated feature for parallel kinematic machine tools. To reach this point, further studies regarding the control integration of force measurement and control features are required as well as the validation of force control with structure-integrated sensors, which is the focus of this contribution.

1.2. Force control with hexapod parallel kinematics

Beside process monitoring and quality assurance, force control is the primary and most challenging field of force measurement. Since the 1970s, force control is a research topic in robotics with an innumerable amount of publications, as outlined in major reviews [37–39] and books [40–43].

Basically, force control strategies can be grouped in *direct* and *indirect* force control [44]. Whereas the later realizes an active compliance through motion control (impedance/admittance control [45,46]) or a passive compliance through a compliant structure (remote centre of compliance [47], flexible joints [48]), the former explicitly closes the force feedback loop and allows to control a desired force value [49]. For stability reasons, direct force control is often based on an inner position or velocity control loop. This motion control loop is usually realized in joint coordinates and implemented in servo drive controllers, which offers a simple way to add force control as outer control loop to existing systems. Necessary transformations between joint and workspace are performed using direct/inverse kinematics (position), the inverse Jacobian (velocity) or the transposed Jacobian (force) [42].

Additional to *pure* force control, *parallel* force/motion control, first presented in [50–52], allows to introduce a nominal position/velocity setpoint at the same time, which can be regarded as feed forward or disturbance rejection value. Obviously, position cannot be controlled in case of contact and force in case of no contact, which has to be taken into account at trajectory/force planning state by the nominal values. Therefore, it is not appropriate to stay in parallel control in all DoF, but rather to select force and motion controlled DoFs. A control scheme providing this, is *hybrid* force/motion control, introduced by [53] and presented in typical implementation by [54]. Depending on the task, natural and artificial constraints, presented by [53,55], are known in advance and used to select force/motion DoF by a selection matrix. Practical realizations can be found foremost in the field of industrial robots, where most recent works include cooperating [56,57] and collaborating [18,58] robots.

Regarding to force control of hexapod kinematics, far less works are available in literature. An adaptive force controlled deburring process for castings has been studied, realized and validated by measurements in [59]. Using a piezo-electric 3 DoF force sensor between end-effector and work-piece, the hexapod is controlled by a deadbeat force controller actuating the feed rate. In [60] parallel force control schemes for a hydraulic hexapod with the goal of controlling a forming process are theoretically studied and evaluated by simulations; following publications [7,61,62] show position control and force measurement. Based on the works of [63–65] a hybrid force/motion control for a hexapod kinematic with linear drives (PALIDA) is presented in [66]. Using a 6 DoF force/torque sensor which is applied at the end-effector, the force control is validated only by detecting and holding a contact. During contact no further movement or process is realized. The also presented milling process is position controlled only. A force controlled thermo smoothing process of milled wood profiles with the hexapod FELIX is shown in [67] by the use of a 6 DoF force/torque sensor between end-effector and tool. During a numerical controlled XY-movement, the Z-direction is force controlled with help of an elastic machine and process model. By the use of a 6 DoF force/torque sensor at the end-effector, [68] presents a contact control of the hexapod Hexa, where especially skill primitives and control laws for all 3 phases (no contact, transition, contact) are developed and validated. Following papers discuss motion and force control of parallel robots with subordinated drive controllers in constrained [69] and unconstrained [70] space addressing control strategies (observer, sliding mode), constraints, an environment model and stability analysis. Further works show force control for specific applications, such as hybrid force control of a hydraulic hexapod for a car axle test rig using a force/torque sensor mounted at the wheel [71], impedance control for assembling tasks [72], or hybrid force/position control of a BOSCH-REXROTH hexapod combined with a second passive measurement hexapod for mechanical NOORU-MOHAMED tests [73]. [74] implemented a Cartesian force control solution on a hexapod using a visual position feed back loop. In soft robotics [75] shows intrinsic force sensing and control for a 3 DoF parallel robot.

Although hexapod structures with integrated force sensors have been used for spatial force measurement and, at the same time, force control solutions for parallel kinematic using FT sensors at the end-effector have been studied, spatial force control of hexapod kinematics using structure-integrated force sensors is not mentioned in the literature. Further, regardless of the sensor system, also force control in 6 DoF with hexapod kinematics as machine tool with numeric control is still a topic of actual research interest with only a few contributions so far. As new contribution, this work presents two methods of force control for a hexapod parallel kinematic, which are implemented and evaluated with both, conventional and structure-integrated force sensors, proving the latter to be compliant with the performance requirements. Further, the software integration into the commercial numeric control software system BECKHOFF TwinCAT as well as a G-Code integration is presented, which allows to control the developed solution by a widespread language.

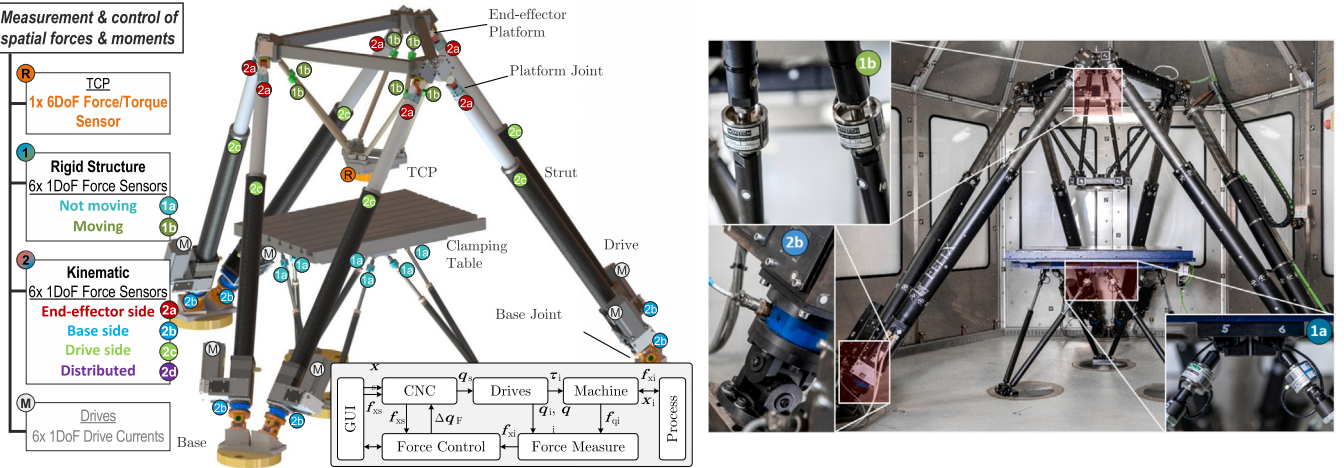


Fig. 1. Structure-integrated force measurement in hexapod structures and kinematics: Left approach and sensor placement; 1a: Rigid not moving hexapod structure (e.g. clamping table), 1b: Rigid moving hexapod structure (e.g. end-effector platform), 2a-d: Hexapod kinematics with sensors in the struts at various positions, where 2d is any mixture of 2a-2c and not displayed; Right: 1b: end-effector with integrated force sensors used in this contribution [5].

2. Approach

Spatial hexapod force control with structure-integrated force sensors bases on the approach of integrated force measurement for parallel kinematics that is presented in previous contributions [1–5,36]. Fig. 1 left summarizes 5 ways of force sensor integration and 2 standard solutions (R: 6 DoF FT sensor, C: drive measurement) as reference. For each integrated sensor system, six 1 DoF force sensors are placed within the hexapod structure or kinematic, where the rigid structure can be not moving (1a) or moving (1b), and the hexapod kinematic allows for different sensor positions (2a-d). For all setups, machine and process induced influences need to be compensated for to achieve an accurate measurement, which is performed by an control-integrated model. Based on a proof of concept for all setups presented in [1,2] gives a more detailed view on the end-effector including the dynamic model as well as accuracy and precision analyses during quasi-static, dynamic, and milling process force measurements. As every model needs a parametrization and some of the model parameters can change during machine usage, parameter identification procedures are studied in [4]. Further, evaluations regarding stiffness changes are discussed in [3,36].

This contribution presents a hybrid/parallel force control of the hexapod machine tool using the rigid hexapod-shaped clamping table (1a), the rigid hexapod-shaped end-effector (1b), the hexapod kinematic with sensors above the base joints (2b) as well as the commercial FT sensor as reference (R), Fig. 1.

In order to realize force control for a numerical controlled machine tool, different use cases with different requirements regarding control functions are shown in Table 1.

The implementation of direct force-controlled teach-in (UC1), which is commonly used as user-guided programming technique, requires an explicitly closed force control loop with selectable coordinates and basic safety functions. Since a parallel numerically controlled motion is not intended, neither hybrid nor parallel force controller structures are required, and, as the nominal forces are always zero, no interface for force set-point application is necessary. In consequence, this is the simplest use case regarding control integration that, further, requires only an asynchronous Programmable Logic Controller (PLC) task with real-time but moderate clock rate.

Environmental interaction with constant or asynchronously given force set-points (UC2), e.g. for grinding or polishing applications, requires further implementations to search and manage the contact as well as programmable task frames and a simple interface that allows force set-point application.

Finally, some processes require varying process forces (UC3) that need to be interpolated synchronously to the CNC movement. To this end, full G-Code-based control and set-point application is required as well as hybrid/parallel control schemes and real-time calculation within the interpolator (IPO) cycle.

From UC1 to UC3, the use cases require a more and more complex architecture and deeper integration into the control system but, on the other hand, provide more features. Based on the force measurement task, meaning the acquisition of actual forces from multiple structure-integrated sensors and their processing to Cartesian forces in the Task Space by a control-integrated measurement model in real-time, the force control task needs to implement additional interfaces. Hereby, the methods to acquire nominal forces from the user and to apply force controller generated offsets to the drives synchronously are crucial.

To meet the needs of all use cases, two implementation approaches are presented that vary in terms of complexity and offer different features. The main difference is in the way how user inputs are injected into the control system.

LR1 In the first solution, the force control offsets are applied to the position-based drive controllers by a PLC via the CNC by the use of a proprietary CNC-PLC interface. The nominal forces are fed asynchronously by an external non-real-time programme in user space to the PLC. This allows to realize the use cases teach-in (UC1) and force control with constant/asynchronous input (UC2).

LR2 In the second solution, the nominal forces are acquired and interpolated synchronously to nominal positions using G-Code-functionality with the help of virtual force axes, which is more invasive than LR1. This enables to realize use case UC3. Further, the force control offsets are applied to the drive controllers by a man-in-the-middle-approach without the knowledge of the CNC.

Before presenting the force control solutions, basics of the force measurement and the measurement models can be found in Section 3. Section 4 discusses force control strategies and the two mentioned specific solutions, which have been realized on the hexapod machine tool FELIX I with structure-integrated force sensors and a commercial numerical control. Finally, both solutions are validated by experimental studies containing teach-in and contour following setups in different variations, as presented in Section 5.

3. Force measurement models

Force measurement with structure integrated force sensors is topic of previous contributions [1,2,4,5]. However, since understanding the

Table 1

Use cases of force control and requirements to the control system.

Use-Case	Description	Required functions (cumulating)	Real-time
UC1	Force-controlled teach-in	-Direct force control -Boundary check -Coordinate selection	Moderate PLC-Clock (2–20 ms)
UC2	Force control with constant or asynchronous force set-point	-Hybrid force control -Task frames -Contact search and offset control -Simple force set-point application	Moderate PLC-Clock (2–20 ms)
UC3	Force control with synchronously interpolated forces and positions	-Hybrid/parallel force control -Synchronous force set-point application -State control via G-Code -Parameter control via G-Code	High IPO-Clock (1–4 ms)

force measurement is essential for the force control with structure-integrated sensors, some background shall be given to the reader, especially, with regard to the measurement models.

In order to compensate for machine and process induced influences from force sensor signals and achieve an accurate measurement, all presented measuring systems require a measurement model. Depending on the exact sensor placement, Fig. 1 left, different influences need to be included into the model. The larger the distance between TCP and sensors within the machine structure, the more system parameters as well as online-calculated machine states need to be taken into account.

3.1. Clamping table – 1a

For non-moving rigid bar structures, the measurement model calculating the searched external Cartesian (process) forces ${}^A f_{\text{Ext}} = \{f_x, f_y, f_z, m_x, m_y, m_z\}$ from the measured sensor forces f_q simply requires the geometric transformation of the forces using the geometric Jacobian \mathbf{J}_T of the rigid sensor framework and the introduction of six zero-offsets of the sensors f_{q0} for a simple taring

$$\begin{aligned} {}^A f_{\text{Ext}} &= {}^A \mathbf{X}_T^F \mathbf{J}_T^{-T} (f_q - f_{q0}) \\ &= {}^A \mathbf{X}_T^F \begin{pmatrix} \mathbf{n}_1 & \cdots & \mathbf{n}_6 \\ \mathbf{h}_1 \times \mathbf{n}_1 & \cdots & \mathbf{h}_6 \times \mathbf{n}_6 \end{pmatrix} (f_q - f_{q0}). \end{aligned} \quad (1)$$

Hereby, \mathbf{n}_i represent the unit vector that expresses the direction of force sensor i and \mathbf{h}_i is the corresponding lever with respect to the table base frame $\{T\}$ [4]. With the help of the spatial force transformation

$${}^A \mathbf{X}_T^F = \begin{pmatrix} {}^A \mathbf{R}_T & \mathbf{0} \\ S({}^A \mathbf{o}_T) {}^A \mathbf{R}_T & {}^A \mathbf{R}_T \end{pmatrix}, \quad (2)$$

the result is transferred to the desired output frame $\{A\}$ using the displacement ${}^A \mathbf{o}_T$ and the rotation matrix ${}^A \mathbf{R}_T$ [76].

Consequently, this measurement model includes 6 equations, 36 constant parameters for the Jacobian \mathbf{J}_T and 6 quasi-constant parameters to tare the sensors using f_{q0} .

3.2. End-effector platform – 1b

A moving rigid bar hexapod structure with integrated force sensors, such as the end-effector platform, does at least require a dynamic model of the rigid body dynamics of the end-effector part that is carried by the sensors. The measurement model in the current form was first presented in [77]. When compared to model 1a, this measuring model includes the additional parameters mass m_p , centre of gravity \mathbf{x}_C , and inertia ${}^P \mathbf{I}_p$ used within the mass matrix \mathbf{M}_p , the Coriolis terms \mathbf{C}_p as well as the gravity vector \mathbf{g}_p in the platform frame $\{P\}$, Fig. 7,

$$\begin{aligned} {}^P f_{\text{Ext}}(\underline{x}, \underline{v}, \underline{\dot{v}}) &= \underbrace{\begin{bmatrix} m_p \mathbf{1} & m_p \mathbf{S}({}^P \mathbf{x}_C)^T \\ m_p \mathbf{S}({}^P \mathbf{x}_C) & {}^P \mathbf{I}_p \end{bmatrix}}_{\mathbf{M}_p} \begin{bmatrix} {}^P \dot{v} \\ {}^P \dot{\omega} \end{bmatrix} \\ &\quad + \underbrace{\begin{bmatrix} \mathbf{0} & m_p \mathbf{S}({}^P \omega) \mathbf{S}({}^P \mathbf{x}_C)^T \\ \mathbf{0} & \mathbf{S}({}^P \omega) {}^P \mathbf{I}_p \end{bmatrix}}_{\mathbf{C}_p} \begin{bmatrix} {}^P v \\ {}^P \omega \end{bmatrix} \end{aligned}$$

$$\begin{aligned} &+ \underbrace{\begin{bmatrix} -m_p {}^B \mathbf{R}_p^T {}^B \mathbf{g}_0 \\ -m_p \mathbf{S}({}^P \mathbf{x}_C)^T {}^B \mathbf{R}_p^T {}^B \mathbf{g}_0 \end{bmatrix}}_{\mathbf{g}_p} - {}^P \mathbf{J}_p^{-T} f_q^* \\ &= \mathbf{M}_p {}^P \dot{v} + \mathbf{C}_p {}^P \dot{v} + \mathbf{g}_p - {}^P \mathbf{J}_p^{-T} f_q^*. \end{aligned} \quad (3)$$

Further, the end-effector pose \underline{x} , velocity \underline{v} , and acceleration $\underline{\dot{v}}$ must be acquired synchronously to the force values and processed in real-time by the model. Finally, f_q^* represents compensated sensor values that already contain corrections f_K and calculates to [4]

$$f_q^* = f_q - f_{q0} - f_K(\underline{x}). \quad (4)$$

Consequently, the measurement model 1b includes 6 equations, 56 constant parameters for the Jacobian (36), sensor offsets (6), sensor corrections (4), and rigid body parameters (10) as well as 18 states to acquire in real-time with the pose, velocity, and acceleration.

3.3. Kinematic – 2a-d

When regarding a hexapod kinematic with integrated force sensors, the whole dynamics including 25 moving bodies need to be taken into account. A suitable approach to separate machine model and measurement model is to correct the measured sensor values f_q by the theoretical sensor forces \hat{f}_q that result from internal loads at the sensor positions [1,5]

$${}^B f_{\text{Ext}}(\underline{x}, \underline{v}, \underline{\dot{v}}) = \mathbf{J}_{\text{Hex}}^T(\underline{x}) (f_q - \hat{f}_q(\underline{x}, \underline{v}, \underline{\dot{v}}) - f_{q0} - f_K). \quad (5)$$

As the difference represents the searched external load, it can be transformed to Cartesian by the, now position dependent, Jacobian of the hexapod $\mathbf{J}_{\text{Hex}}(\underline{x})$. Sensor offsets f_{q0} and sensor corrections, e. g. due to sensor torque sensitivity, f_K are used similar to model 1b.

Depending on the sensor positions, the virtual sensor forces \hat{f}_{q_i} are collected from internal forces at the platform joint ${}^B f_{HY_i}$, spindle nut ${}^B f_{M_i}$, or base joint ${}^B f_{SY_i}$

$$\hat{f}_{q_i}(\underline{x}, \underline{v}, \underline{\dot{v}}) = \begin{cases} {}^B z_{HS_i}^T {}^B f_{HY_i} & \text{Setup 2a} \\ {}^B z_{SS_i}^T {}^B f_{SY_i} & \text{Setup 2b} \\ {}^B z_{SS_i}^T {}^B f_{M_i} & \text{Setup 2c}, \end{cases} \quad (6)$$

where for setup 2d a combination of 2a-2c is used. These internal forces can be taken advantageously from the Newton-Euler model of the hexapod dynamics

$$\underbrace{\begin{pmatrix} \Lambda_{P_1} & \Lambda_{P_2} & \Lambda_{P_3} & \Lambda_{P_4} & \Lambda_{P_5} & \Lambda_{P_6} \\ \Lambda_{V_1} & & & & & \\ & \Lambda_{V_2} & & & & \\ & & \Lambda_{V_3} & & & \\ & & & \Lambda_{V_4} & & \\ & & & & \Lambda_{V_5} & \\ & & & & & \Lambda_{V_6} \end{pmatrix}}_A^{180 \times 180} \cdot \underbrace{\begin{pmatrix} f_1 \\ \vdots \\ f_6 \end{pmatrix}}_f = \underbrace{\begin{pmatrix} b_p \\ b_{V_1} \\ \vdots \\ b_{V_6} \end{pmatrix}}_b, \quad (7)$$

with the equations of motion of the platform part $\{\Lambda_{P_i}, b_p\}$, the strut parts $\{\Lambda_{V_i}, b_{V_i}\}$ and the internal forces of each strut f_i . As the kinematic is parallel, no successive solution is possible and the model result in an equation system with 180 unknowns. Detailed information regarding the measurement models 2a-d can be obtained from the literature [1,5].

Consequently, these measurement models include 186 equations, 260 constant parameters for the rigid body parameters (25x10), sensor offsets (6), and sensor corrections (4) as well as 486 states to acquire in real-time with pose, velocity, and acceleration of each body (25 × 18) and the position-dependent Jacobian (36).

4. Force control

After giving an introduction to force control laws (Section 4.1), this section discusses solutions regarding the injection of the manipulated variables into the numeric control (Section 4.2), the set point specification in G-Code (Section 4.3) as well as the state control of the force controllers (Section 4.4).

4.1. Fundamentals and control laws

A large variety of force control concepts, which differ in characteristics, stability, or implementation, has been studied and presented in the literature, Section 1.2. This contribution neither targets the evolution of force control theory nor the implementation of complex control strategies. Instead, an easy-to-use hybrid/parallel force control shall be implemented into a commercial numerical control system to prove feasibility of structure-integrated force measurement for force control applications. Against this backdrop,

- the existing decentralized joint space cascade control (position, velocity, and current) with attached numerical control shall remain unchanged,
- the force control shall be implemented as explicitly closed *direct force control* loop using the structure-integrated force sensors and the reference FT sensor, respectively, and
- the force control shall run, except for teach-in (UC1), *parallelly* to CNC processing within a user-defined Task Space and only in user-selected coordinates (*hybrid*).

In consequence, the desired approach can be stated as direct position-based hybrid/parallel force/motion control. Hereby, the drives are always in motion control and the force control is superimposed on selected coordinates, when needed. While the set-points for motion ${}^T S \underline{x}_{\text{nom}}$ and force ${}^T S \underline{f}_{\text{nom}}$ are commanded in the Task Space {TS}, the used external input of the CNC requires joint space position offsets Δq_F , as reasoned in Section 4.2.

After calculating the force lags $\Delta {}^T S \underline{f}$ in Task Space with the help of the measured forces ${}^T S \underline{f}_{\text{act}}$, Section 3, and the diagonal *selection matrix* Ξ that allows to specify the actively force controlled degrees of freedom [42]

$$\Delta {}^T S \underline{f} = \Xi \left({}^T S \underline{f}_{\text{nom}} - {}^T S \underline{f}_{\text{act}} \right), \quad (8)$$

different approaches exist to calculate the requested joint space position offsets from the force lag in Task Space: $\Delta {}^T S \underline{f} \rightarrow \Delta q_F$.

At first, the geometric *transposed Jacobian* of the hexapod kinematic $J_{\text{Hex,G}}^T(\underline{x}_{\text{cnc}})$ can be used to define a control law K_{Fq} in joint space

$$\Delta \tau_{qF} = J_{\text{Hex,G}}^T(\underline{x}_{\text{cnc}}) {}^B X_P^F {}^P X_{\text{TS}}^F \Delta {}^T S \underline{f} \quad (9)$$

$$\Delta q_F = K_{Fq} \Delta \tau_{qF}. \quad (10)$$

Even though this control law allows parallel CNC motion and requires low computational cost, it is non-linear with regard to the Task Space and, therefore, excluded.

Instead, only control strategies in Task Space shall be considered, to minimize control deviation, as the manufacturing tasks are defined

in the Task Space. Consequently, a control law K_{Fx} in Task Space shall generate the pose offsets $\Delta {}^T S \underline{x}_F$ in {TS}, which are transformed to the base system {B} straight away

$$\Delta {}^T S \underline{x}_F = K_{Fx} \Delta {}^T S \underline{f} \quad (11)$$

$$\Delta {}^B \underline{x}_F = {}^B X_P {}^P X_{\text{TS}} \Delta {}^T S \underline{x}_F. \quad (12)$$

In the following, three ways are discussed to calculate the joint space position offsets from the Cartesian controller offsets $\Delta {}^B \underline{x}_F \rightarrow \Delta q_F$ by the use of (1) the inverse Jacobian, (2) the full forward and inverse kinematic transformation, as well as (3) the inverse kinematic complemented by a memory.

- (1) The *inverse Jacobian* of the hexapod kinematic allows for the direct transformation of the offsets into joint space

$$\Delta q_F = J_{\text{Hex,A}}^{-1}(\underline{x}_{\text{cnc}}) \Delta {}^B \underline{x}_F. \quad (13)$$

For an appropriate angle format, the analytic Jacobian $J_{\text{Hex,A}}(\underline{x}_{\text{cnc}})$ should be used. As $J_{\text{Hex,A}}(\underline{x}_{\text{cnc}})$ can be obtained from $J_{\text{Hex,G}}(\underline{x}_{\text{cnc}})$, which is calculated in any case during cyclic inverse transformation, the computational costs are very low. In addition, a parallel CNC motion is possible. However, since the Jacobian is calculated for the CNC-pose $\underline{x}_{\text{cnc}}$ but physically depends on the complete machine pose \underline{x} , the result will be inaccurate for large displacements between the CNC controlled pose and the force controlled pose. Nevertheless, with an error of 0.75 μm for $|\Delta \underline{x}_F| = 1$ mm [78], this is a very efficient solution for a force control application with small amplitudes, which apply for many industrial applications. The corresponding signal flow is presented in Fig. 2.

- (2) The second approach uses *full forward and inverse kinematic* transformations (FK and IK) to realize $\Delta {}^B \underline{x}_F \rightarrow \Delta q_F$, as illustrated in the signal flow in Fig. 3. Because only poses can be transformed, the CNC pose ${}^B \underline{x}_{\text{cnc}}$ must be added to the offset, and, since the CNC interpolator outputs only joint space trajectories q_{cnc} , a forward transformation is added beforehand

$${}^B \underline{x}_{\text{cnc}} = FK(q_{\text{cnc}}) \quad (14)$$

$$\Delta {}^B \underline{x}_{\text{cmd}} = {}^B \underline{x}_{\text{cnc}} + \Delta {}^B \underline{x}_F. \quad (15)$$

Again, the angle format must be recognized, here the offset orientation is expressed as rotation matrix before addition using the RODRIGUEZ equation [79]. Finally, inverse transformation produce the commanded joint space coordinates q_{cmd} that can, if necessary by the interface, be reduced to joint offsets Δq_F by subtracting q_{cnc}

$$q_{\text{cmd}} = IK({}^B \underline{x}_{\text{cmd}}) \quad (16)$$

$$\Delta q_F = q_{\text{cmd}} - q_{\text{cnc}}. \quad (17)$$

Fig. 3 shows the signal flow of this approach.

- When compared to method (1), method (2) guarantees full precision all over the work space, and also allows parallel CNC positioning. As both, FK and IK, are required within every interpolator cycle in real-time, this method implies high computational costs.
- (3) By the use of the *inverse kinematic and a memory*, expressed by Z^{-1} , an incremental movement relating to the last pose can be realized

$${}^B \underline{x}_F = Z^{-1}({}^B \underline{x}_F) + \Delta {}^B \underline{x}_F \quad (18)$$

$$\Delta q_F = IK({}^B \underline{x}_F) - q_{\text{cnc}}. \quad (19)$$

This allows to use the full inverse kinematic without the costly forward transformation that has to be calculated only once after initialization. However, in this approach all hexapod movements result from the force controller offsets, which forbid a parallel CNC positioning.

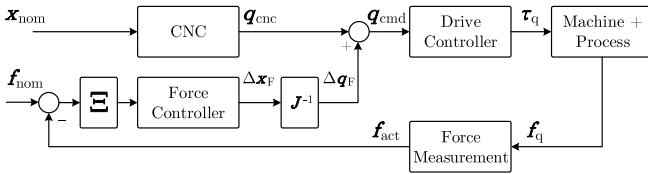


Fig. 2. Signal flow of force control using the inverse Jacobian approach.

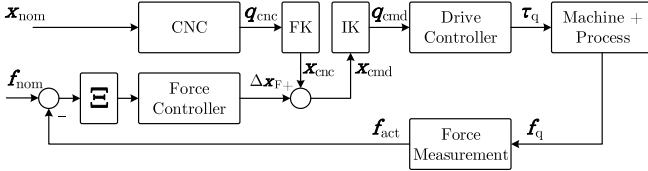


Fig. 3. Signal flow of force control using full forward/inverse kinematic.

All three approaches have been successfully implemented and tested at the parallel kinematic machine tool FELIX I. Still, their ability to fulfil the desired use cases, as presented in Table 1, vary: Regarding teach-in operations (UC1), method (3) is particularly suitable, as it allows user-guided movements through the workspace with a simple implementation (no environmental contact, no nominal force: $f_{\text{nom}} \equiv 0$). The forbidden and, therefore, impossible parallel CNC-based positioning, $q_{\text{cnc}} \equiv \text{const.}$, is not of importance for this use case. For force control applications that require only small offsets Δx_F (UC3 with feed forward of the workpiece contour), method (1) can fulfil the requirements in providing an implementation with low computational costs, where the positioning error is small. Finally, if enough computing power is available, method (2) can be regarded as preferred solution, since it enables all use cases. Beside teach-in and hybrid/parallel force/motion control, also use cases with unknown workpiece contour and, therefore, significant force controller induced positioning offsets Δx_F are applicable. As high computational costs usually entail high financial costs, the methods (1) and (3) provide simple and cheap solutions for less demanding use cases.

Regarding the choice of K_{Fx} , a simple PID controller is used in this contribution

$$K_{Fx} = \frac{X}{F} = K_P \left(1 + \frac{1}{sT_N} + \frac{sT_V}{1+sT_1} \right). \quad (20)$$

More advanced controller structures are also applicable for the approach. However, this work mainly focus on the integration of force measurement and control into a commercial numerical control, as described in detail in the next sections.

4.2. Injection of manipulated values

For the implementation of the force control, the manipulated signals Δq_F calculated by the force controller must be applied within the control system to the current, numerically controlled movement. The control system BECKHOFF TWINCAT 3.1 offers interfaces that mainly have been created for other applications, such as NC streaming, manual operation, dynamic coordinate systems, external commanding of the axes, or user-defined coordinate transformations. NC streaming is regarded as inappropriate due to the unsuitable playback behaviour for closed-loop control and the missing possibility for parallel motion by the CNC. The manual operation is excluded due to the single-axis control only and not supported parallel CNC movement, and, finally, the dynamic coordinate systems are dismissed due to the resulting displacement of the force-controlled relative to the position-controlled coordinate system. Also excluded is the integration of the force controller into the transformation because of the difficulty to guarantee a consistent direct and inverse kinematic system at any time. This leaves two

options for manipulated values injection: the external commanding of the ControlUnits in the CNC via the proprietary High Level Interface (HLI) and the integration of the C++ force controller module between CNC and drives in the sense of a ‘man-in-the-middle’ intervention, which respectively form the basis of the two implemented solutions LR1 and LR2 of the force control that are presented next.

Approach LR1 uses the High Level Interface for external commanding of the axes. A PLC created for this purpose receives internal (via the process image) or external (via the ADS interface) set-points and forwards them after preprocessing as axis offsets to the ControlUnits of the CNC, Fig. 4. Advantages of this approach are the direct application of position and speed offsets to the drives as well as the possibility of parallel CNC operations. At the same time, the direct application of the offsets is disadvantageous, since neither safety monitoring nor path planning or synchronization can be done by the CNC. Therefore, a separate trajectory planning including limit value monitoring (position, velocity, acceleration, jerk) and interpolation to the position control is necessary and has been implemented, in order to prevent set-point jumps on the axes. This provides the possibility to process strongly asynchronous, non-real-time inputs: Thus, an interface in user space can receive position or velocity set-points from other devices, such as cameras, joysticks, or gamepads, and write them asynchronously to the PLC. If no new set-points are received or if the communication breaks down, the last values and, thus, the position, are held. First results are demonstrated in [78,80], and in [81] the interface is used for online correction of thermally induced errors by means of a structural model on the MINIHEX parallel kinematic.

Although the applicability of the interface for force control for the use cases UC1 and UC2 can be confirmed in principle, some deficiencies are noticeable, which in particular affects use case UC3. As main aspect, it is not possible to apply the offsets synchronously to the CNC movement: While the set-points for positions are still specified in the G-Code, force set-points must be specified separately. After the position set-points have been preprocessed by the CNC path planning and interpolation and the force set-points have been processed into joint position offsets by the force controller, the exact time at that the offsets are applied to the ControlUnits is undefined and, thus, a synchronous parallel force/position control is not applicable. Therefore, the approach is mainly suitable for force control without set-point (teach-in, UC1) or with constant or asynchronous set-point (UC2). In addition, long processing times and dead times caused by the additionally required PLC task as well as the required path planning lead to poor performance, so that the response time of the force control is rather high [78].

Finally, the connection via the HLI requires the implementation of the solution as a PLC, since the HLI is not available in C++. On the other hand, the present C++ libraries, including the kinematic transformation, are not available for the PLC. This leads to an obligatory set-point specification in axis coordinates also for the PLC and, as a consequence, that both kinematic transformation and force transformation must be carried out in the preprocessing, which complicates the implementation of the task coordinate systems.

Due to the deficiencies described above, in particular the delay times and the lack of a completely synchronous processing of position and force inputs, a second variant of the force control has been developed and investigated [5,82]. *Approach LR2* allows in combination with the improved set-point specification, presented in the next section, the realization of use case UC3 and is intended as a ‘man-in-the-middle’ setup, since the force controller contains a C++ module that is placed between the CNC and the drive controller: The force controller module appears for the CNC like a drive controller and for the drive controller like a CNC, Fig. 5. For this purpose, set-points and actual values as well as control and status word are manipulated and forwarded accordingly. A replacement of the cascade controllers is deliberately not carried out, since they are located in the servo drives, which results in smaller cycle and dead times (current controller: 125 µs, velocity controller: 250

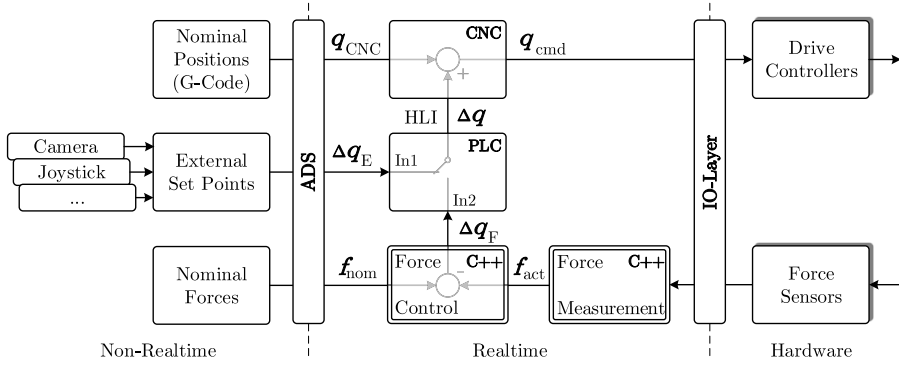


Fig. 4. Principle of approach LR1 [5].

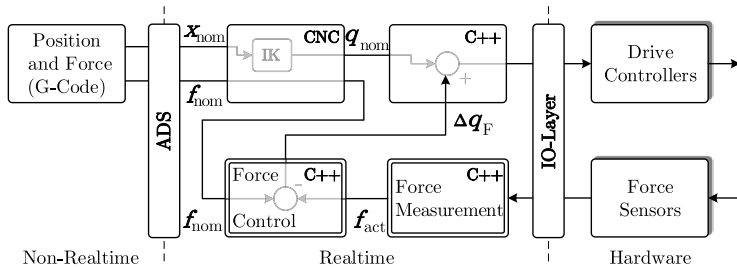


Fig. 5. Principle of approach LR2 [5].

μ s, position controller and SERCOS II: 1 ms). By integrating the C++ module into the CNC GEO task, task limits and additional dead times are avoided during implementation.

However, also LR2 has some disadvantages: For example, path planning, interpolation, and safety checks of the commanded offsets are not carried out by the CNC, since the connection is made after CNC processing. In addition, the tracking error monitoring must be deactivated within the CNC, because the CNC does not know the commanded offsets, but does know the correct actual values. The monitoring in the inverters remains active and guarantees safety.

At the same time, there are significant advantages, when compared to connection via HLI in LR1: First of all, path planning and interpolation of the CNC can be used for nominal force and position values at the same time, if the set-point specification is realized via virtual additional axes directly from the NC programme, as presented in the next section. Further, the solution does not require an additional PLC, but can be implemented entirely in C++ using the existing libraries, such as the inverse kinematics and the limit value check of the working space. Due to the real-time synchronous connection to the force controller, an additional path planning of the offsets is not required. Consequently, synchronous set-point input and processing is guaranteed, and significantly higher dynamics can be achieved.

4.3. Set-point specification in G-code

The possibilities, characteristics, and limits of the set-point specification for position and force differ for the two solutions LR1 and LR2, presented in the last section. For LR1, with injection of the manipulated values using HLI, the motion is specified via G-Code to the CNC and the force input via a separate interface (ADS) to the C++ module of the force controller. Consequently, the set-points for position and force are asynchronous to each other. The path planning allows the processing of asynchronous and non-smooth external set-points, e.g. for other practical applications, such as tracking control, but, at the same time, significantly slows down the processing in the sense of a closed-loop control, and, also, does not ensure synchronous processing

of the set-points. For this reason, the realization of the use case UR3 (process force control with variable set-point force and synchronous force /position control) is not possible with the solution LR1. However, the synchronous set-point specification of force and motion is a prerequisite for the force-controlled machining of many practical components because only then it is possible to vary the magnitude and direction of the force during machining.

Therefore, the aim is to programme the hybrid/parallel force control task in one NC programme by means of G-Code in accordance with DIN 66025 / ISO 6983 as a practical and well-known programming format. Possible solutions for the used BECKHOFF TWINCAT 3.1 control system are the use of M commands with variables, user-defined external variables, or virtual axes for the force coordinates. Only the latter one, the integration of force axes in the same CNC channel as the positioning axes, guarantees full synchronous interpolation of all set-points. With the implementation of the LR2 solution, six physical positioning axes {X, Y, Z, U, V, W} and six virtual force axes {XF, YF, ZF, UF, VF, WF} are available for one NC block, Fig. 6.

As described above, drive variables for the real axes, such as status word, control word, or actual values, are forwarded by the C++ module. For the virtual force axes some additional drive parameters, e.g. the SERCOS phase, are simulated and the actual force values from the force module are fed back to the CNC. For this purpose, the force axes can be switched to tracking mode in the state 'position control' to ensure correct display of the actual force by means of the virtual axes on the HMI.

Finally, the CNC can be used for monitoring of the actual forces, as the force sensors feed back their actual values to the virtual force axes of the CNC. In contrast to position axes, some modifications are made to suit the deviating requirements of force control: Force lag is only to be supervised when the machine is in contact. If contact is not established, all force axes are set to follow up mode, which disables lag monitoring. Axes that are not selected for force control have to be put into follow up mode as well. The precision stop window feature of the CNC can be used to coordinate the parallel force and position commands specified in the NC-file.

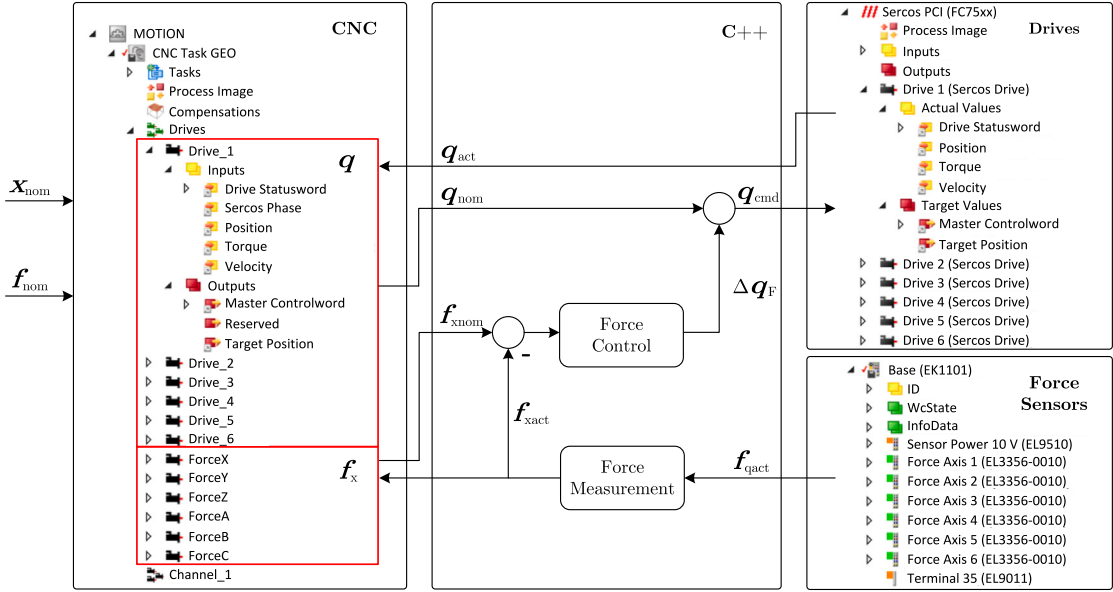


Fig. 6. Solution LR2 in detail with synchronous position and force set-points from G-Code using real position and virtual force axes as well as a ‘man-in-the-middle’ C++ setup [5].

One prerequisite for the synchronous G-Code usage is the integration of the kinematic forward and backward transformation into the CNC core. These transformations are already available as real-time capable C++ code with the work on the force measurement [1,2,36] and are adapted according to the BECKHOFF transformation interface ‘McCOM-Trafo’ with the help of the functions *Forward* and *Backward*

$$x = \text{Forward}(q) \quad (21)$$

$$q = \text{Backward}(x). \quad (22)$$

In addition, the necessary parametrizations of the NC kernel are made: different angle representations (EULER, KARDAN, BLD) are taken into account by transformation types (#KIN ID 65, 66, 67) as well as appropriate functions that check the compliance with machine limit values (position, speed, acceleration, joint angle, etc.) and cycle times to guarantee real-time. This allows the machine to be controlled by means of G-Code in Cartesian coordinates x by activating the kinematic transformation in the core (#TRAFO ON), Table 2.

Due to the inherent interdependency of machine and environment during force controlled tasks, the precise definition of nominal force values depending on the task is important. To facilitate the programming of such tasks, a set of coordinate systems can be defined by the user that apply for both, position and force values. These user-defined coordinate systems are integrated into the kinematic transformation and the G-Code with 12 parameters that define the Task Base ${}^B T_{AB}$ (fixed to base) and Task Platform ${}^P T_{AP}$ (fixed to platform), Fig. 7. The conversion between programmed coordinates T_{NC} and machine coordinates ${}^B T_P$ is carried out for the poses by

$$T_{NC} = {}^B T_{AB}^{-1} {}^B T_P {}^P T_{AP} \quad (23)$$

$${}^B T_P = {}^B T_{AB} T_{NC} {}^P T_{AP}^{-1}. \quad (24)$$

and for the forces at the end-effector by

$${}^F X_P = {}^P T_{AP} {}^F X_B {}^B f_{Ext} \quad (25)$$

$${}^B f_{Ext} = {}^B X_P {}^P T_{AP} {}^F X_B f_{NC}. \quad (26)$$

Analogous to the provision of the force measurement functionalities in the G-Code, control functions and further parameters are made available for the force control with the help of M-commands and user-defined external variables in the NC programme, Table 2. These include the basic functions, such as starting and stopping the force control,

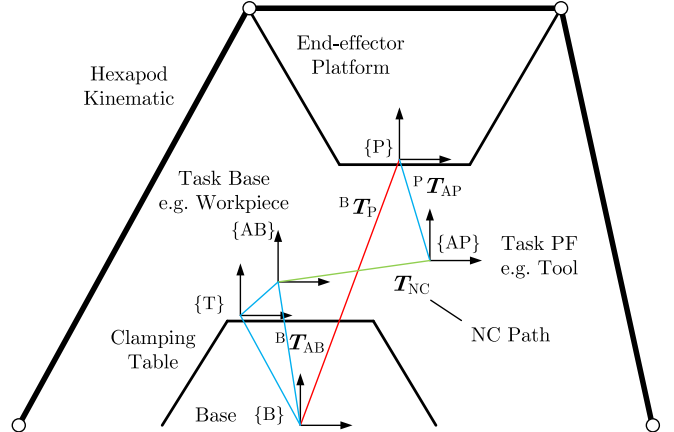


Fig. 7. Order of the main coordinate frames.

the selection of the force-controlled coordinates with the help of the selection matrix Ξ and the definition of the task coordinate systems mentioned above. In addition, there are numerous other parameters, such as safe workspace limits for active force control, ‘soft’ and ‘hard’ controller parameters (K_p , T_n) for each of the six degrees of freedom as well as coordinates of the origin for control in radial coordinates and control commands, or de-/activation of the variable task space as well as, for example, control in radial or normal direction, Section 5.

Finally, Listing 1 shows an example for the use of the force control in G-Code: A base coordinate system rotated by $C = 30^\circ$ is defined, the force control in -Z direction is selected by the selection matrix, the kinematic coordinate transformation in EULER angles is activated, and the start position $x_s = \mathbf{0}$ is approached. Subsequently, the force control with automatic contact search is activated, a force of 100 N is built up and, finally, during the travel from $X = 0$ mm to $X = 500$ mm, the force in -Z direction is increased from 100 N to 300 N. In parallel, the Z-position is controlled by feed-forward from $Z = 0$ mm to $Z = 10$ mm.

In summary, the LR2 solution with set-point specification in G-Code using real positioning and virtual force axes as well as a ‘man-in-the-middle’ C++ module for actuating variable connection offers numerous advantages for force control: Force and position set-points are interpolated synchronously, dead and delay times are significantly reduced

Table 2

G-Code commands for sync. position and force control.

G-Code	Description
X, Y, Z, U, V, W	Positions \underline{x}_s/q_s (#TRAFO ON/OFF)
XF, YF, ZF, UF, VF, WF	Forces f_{xs}
#TRAFO ON/OFF	En-/disable kinematic transformation
#KIN ID[Trafo]	Choose type of kin. transformation
.PARAM[1..6]	Define task frame Base ${}^B T_{AB}$
.PARAM[7..12]	Define task frame Platform ${}^P T_{AP}$
.PARAM[13..18]	Select force controlled coordinates Ξ
.PARAM[19..30]	Set workspace limits $\underline{x}_{\min}, \underline{x}_{\max}$
.PARAM[31..54]	Set controller parameters K_p, T_n
.PARAM[55..57]	Set origin for radial/normal control
M50, M51	Start/Stop force control
M52, M53	Choose 'soft' or 'hard' parameters
M54, M55	En-/disable variable task space
M56, M57	Activate radial/normal force control
M58	Start teach-in

Listing 1: G-Code example for hybrid force/position control

```

N00 #TRAFO OFF      ; Disable kinematic transformation
N05 #KIN ID[65]     ; Select Euler angles
N10 V.G.KIN_STEP[0].ID[65].PARAM[6] = 30 ; Turn C by 30°
N15 V.G.KIN_STEP[0].ID[65].PARAM[15] = -1 ; -Z force dir.
N20 #TRAFO ON       ; Enable kinematic transformation
N25 G1 X=0 Y=0 Z=0 U=0 V=0 W=0 F50 ; Goto 0 w. 50 mm/min
N30 M71             ; Tare force sensor
N35 M51             ; Search contact
N40 G60 ZF=100      ; Control force to ZF=100 N
N45 G1 X=500 Z=10 ZF=300 ; Move X=500, Z=10, Force ZF=300 N
N50 M50             ; Disable force control
N55 M30             ; Program end

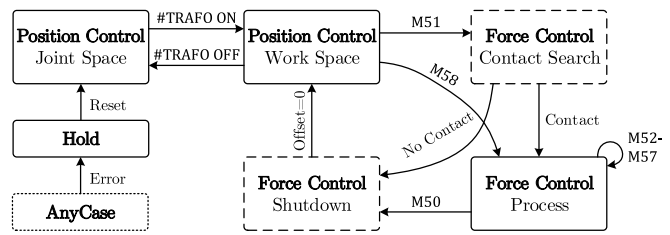
```

by task integration and the absence of path preparation, and the set-point specification is carried out uniformly using a known, standardized programming language. For the connection of asynchronous external set-points, e.g. from cameras or joysticks, which cannot be realized with LR2, as well as for teach-in, the LR1 solution is available and can co-exist with LR2 on one control system.

4.4. State control

The hexapod can be used with and without force control. When in pure position control, occurring contact forces are not taken into consideration. Controlling forces is only possible when the machine is in stable contact. Therefore, force control requires a state control according to the physical states (no contact, possible contact, and contact) that coordinates the contact search in the direction selected by the user, the activation and deactivation of the force control, or the handling of errors. This is realized by a state machine implemented in the C++ module of the force control, which is triggered by corresponding M commands in the G-Code for the solution LR2, Fig. 8. By default, the CNC operates in the joint space with kinematic transformation in the user interface (#TRAFO OFF). However, as described in the last section, the interpolation in workspace coordinates is a prerequisite for the synchronous set-points of position and force in the G-Code, so that the force control can only be activated if the kinematic transformation in the kernel is active (#TRAFO ON). This is called 'Position Control Workspace' in the state graph, even though the actual position control still takes place in the joint space by the decentralized joint controllers in the servo drives and only the interpolation takes place in the working space.

After activation of the process force control (M51), a contact search is performed to establish the contact situation with the environment desired by the user. The contact search is speed-controlled in the directions selected in the selection matrix Ξ until an application-dependent contact force is reached. It is aborted, however, if no contact is found

**Fig. 8.** Statemachine used for managing the transition between position and force control [5].

after a defined distance or if a force occurs in a non-selected direction. For teach-in (M58), contact search is skipped.

When the 'Force Control Process' state is entered, the force controllers are finally activated for the selected directions and the force set-points programmed in the G-Code are fed through to the force controllers. All structure-integrated force measurement systems are available as a source for the actual force values. Algorithmically, for the position-based force controllers, normal PID controllers are used for each active degree of freedom $i = 1 \dots 6$, Eq. (20).

The controllers are supplemented by filters and the controller parametrization can be adapted by the user in the G-Code (PARAM[31–54]). Furthermore, different parameter sets are available, which can be switched between via M commands (M52, M53). By integrating the override into the force controller, the machine operator keeps the force-controlled movement under control at all times in addition to the position-controlled movement. Finally, a variable taskspace can be activated for tasks in which the direction of the process force changes during the process (M54, M55).

Force control is implemented for radial (M56) and normal (M57) direction. In the first case, the user sets a fixed point in the taskspace (PARAM[55–57]), which defines with the variable end-effector position the desired force direction. Ideally, the fixed point defines the centre of a circular path, which causes the taskspace to be rotated in such a way that the process force always acts towards the centre of the circle. In the case of force control in normal direction, the process force is aligned normal to the workpiece surface. The activation is based on radial control and is only possible if the process force is sufficiently large and stable. During the force control, a safety monitoring is permanently active, which stops the traversing movement at the defined workspace limits (PARAM[19–30]) or in the case of transverse forces in non-selected force directions [82].

To end the force control (M50), the resulting offset to the CNC position ${}^A \underline{x}_F$ must be reduced in a controlled manner in order to be able to continue with position control without interrupting the NC programme. This is done in the state 'Shutdown' analogue to the contact search in a speed controlled manner and is also necessary for teach-in mode. Finally, an error state 'Hold' is used to react in case of unforeseen events and errors to stop the machine. Since the offset cannot be reduced in this case, this state can only be left by a CNC reset. Some of the CNC-internal states and control commands necessary for the state control are only available in the commercial control TWINCAT 3.1 via the so-called high-level interface, which is why they have to be forwarded to the C++ module of the force control via a PLC. This applies, for example, to the status of the kinematic transformation, the switching of M-commands or the de-/activation of the tracking mode. Other parameters, such as the user-defined coordinate systems, are only available via the C++ interface of the kinematic transformation and are also forwarded from there to the force control. Since these detours only affect the state control and parametrization, there are no delay times for the control. Finally, there is also a connection to the C++ module of the force measurement for the integration of the preprocessed measurement models into the control loop.

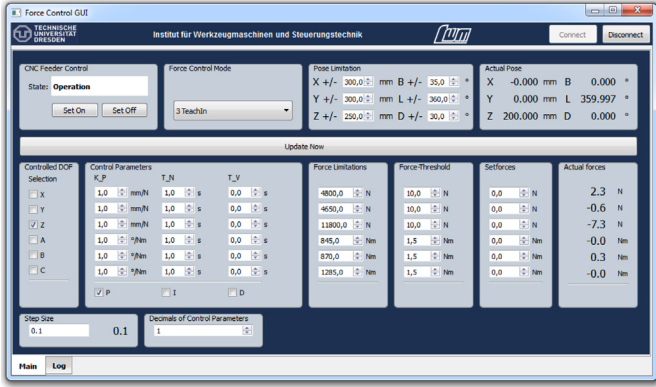


Fig. 9. User interface of solution LR1 that allows to choose force controlled coordinates, controller parameters, constant force set-points as well as limits for workspace and forces [78].

5. Implementation and validation

Validation and Evaluation of the two presented solutions are carried out with respect to the ability to realize the use cases introduced in Table 1. In the following sections, the results are presented on the basis of the use cases UC1 Force-controlled Teach-in (Section 5.1), UC2 Asynchronous Contact Force Control (Section 5.2) and UC3 Motion-synchronous Force Control (Section 5.3). Finally, the structure-integrated force measurement systems are investigated and compared with regard to their suitability for force control (Section 5.4).

5.1. Force-controlled teach-in

Solution LR1 implements the use-case UC1 and allows the operator to conveniently set the relevant operating modes and parameters by means of a user interface, Fig. 9. Thus, the force-controlled coordinates ('Controlled DOF') and the underlying controller (P/I/D) can be selected with individual parameters ('Control Parameters') as well as limit values for force ('Force Limitations') and working space ('Pose Limitation') or force threshold values ('Force Threshold'). 'Actual Pose' and 'Actual Forces' are permanently displayed to the operator, and, finally, it is possible to set nominal forces that are constant until the next operator input. [78]

For this application, the path planning integrated in LR1 is of great advantage, since it realizes a continuous movement of the end-effector that feels smooth and controllable for the operator. The lower dynamics is of no consequence due to the missing force set-points, the lack of ambient contact, and the absence of NC movement. Likewise, the operator interaction of the solution LR1 by means of a user interface is also better suited for this application than the G-Code control of the solution LR2.

On the modelling side, a correct and aligned measurement model is a prerequisite for all force measurement and control applications. However, this is particularly relevant for force-controlled teach-in, since otherwise the machine may drift if there is no operator input. With the parameter identification procedures presented in [4], the correct model parametrization for all measurement models can be found in a few seconds. With a parametrizable threshold of the force control, smaller parameter uncertainties and sensor drifts can be taken into account and a standstill window can be realized.

Consequently, the applicability of the structure-integrated force measurement in moving components for force-controlled teach-in has been demonstrated. At the same time, integrated force sensor technology by measuring forces within the structure proves to be particularly advantageous: While the force measurement platform at the end-effector (*R*) allows teach-in only when the end-effector is touched,



Fig. 10. Force-controlled teach-in of the Hexapod FELIX I using solution LR1 and structure-integrated force sensors in the hexapod struts (2b) [83].

the integrated sensors in the end-effector platform (1b) make it possible to guide the machine by touching the platform, and, finally, sensors in the struts (2b) even make guiding on the struts or the upper part of the platform possible, Fig. 10. As the distance from the user interaction point to the TCP increases, so does safety and comfort for the operator.

5.2. Asynchronous contact force control

The contact force control with constant or asynchronous set-point force (UC2) allows the realization of applications, such as force-controlled grinding, polishing or deburring, where the synchronicity of the set-point values for force and motion in the real-time context is not a condition. As a prerequisite, the machine must be brought into contact with the environment in a controlled manner and the control system must enable direct hybrid process force control of an externally pre-definable set-point force. Therefore, in addition to the functions required for UC1, contact search, state control, and a simple interface for asynchronous force set-point specification are required for practical applications, Fig. 4.

The suitability of the LR1 solution approach and the structure-integrated force sensor technology for asynchronous contact force control is tested in [78]. With a test arrangement consisting of a heavy-duty roller (tool) mounted on the end-effector and a steel sheet (workpiece) fastened to the frame, various functions, summarized below, are carried out. The following summarized experimental investigations are carried out to validate and evaluate the force control.

First of all, after a contact force of 500 N has been established, the basic operation of direct force control in the contact is demonstrated by means of nominal and disturbance step of ± 500 N in the Z direction. For this purpose, the set-point force is specified manually via the user interface and the disturbance force is applied by specifying a positioning movement in the Z direction. The parameters of the PID controller are set in advance according to the contact compliance. This results in control overshooting of 3.6% (to 1000 N) and 24.2% (to 500 N) for the nominal steps and up to 100% for the disturbance steps. Further, due to the high dead and delay times of the manipulated variable feed-forward control and integrated path planning, long settling times of up to 260 ms until the control deviation falls below the 5% band [78].

On this basis, hybrid force control has been implemented and validated by comparing position- and force-controlled motion with mounted heavy-duty roller on the steel plate attached to the frame. A cyclic traverse movement is performed with a travel distance of 200 mm in X-direction and a travel speed of approx. 3.5 m/min and a constant nominal force of 1000 N in the Z-direction, during which, without force control due to the uneven clamping, interference forces of up to ± 300 N occur. With activation of the force control in Z-direction, the target force is maintained with remaining disturbing forces of approx. ± 20.5 N (single standard deviation), which corresponds to a

remaining uncertainty of approx. 6.2% (3 s, 99.73%). This test basically proves the functionality of the force control, but at the same time, with significant force peaks at the reversal points, it again shows weaknesses in the dynamics [78].

The reason for the low dynamics is mainly assumed to be the mechanism of the manipulated variable feed-forward of the LR1 solution. For this reason, the dynamics of the interface is evaluated by a manipulated value step at the force controller output of the C++ task of $\Delta q_{IF} = 1$ mm. After the path preparation in the PLC task, the offset is added to the position set-points in the CNC GEO task and finally realized by the position control in the inverter. In relation to the actual value, this results in a dead time of $T_d = 22$ ms, a settling time of $T_{95} = 120$ ms and, with the reversing tangent method, the delay dead time $T_u = 29$ ms and the compensation time $T_g = 64$ ms. The high dead time results mainly from the implementation of the solution in several successively running tasks (C++, PLC, CNC). With a cycle time of $T_0 = 2$ ms, two cycles pass with $T_{d1} = 4$ ms until the path is available and a total of long $T_{d2} = 12$ ms or 6 cycles, until the set-point leaves the controller. If the measuring time of 4 ms is taken into account, the actual value is already present at the encoder after 18 ms [78]. As a result, the asynchronous contact force control with the LR1 solution is considered validated, but in this case the achievable dynamics is rather low due to the required path planning and the high dead times. This is a disadvantage for the contact force control, in contrast to the application case of teach-in, due to stability because the controller gain is limited and the stability limit is lowered.

5.3. Motion-synchronous force control

The force/position control with motion-synchronous set-point specification according to use case UC3 is implemented with the solution LR2 approach by the ‘man-in-the-middle’ setup (Section 4.2) and the integration of virtual force axes into the CNC and G-Code (Section 4.3). Thereby, the solution approach allows the integration of further functions, such as feed-forward control of movements in force direction (hybrid and parallel control) or variable task coordinate systems, which are implemented within the scope of the work [82] and validated by extensive experimental investigations. With the elimination of task boundaries and internal path planning, the LR2 solution approach also overcomes the deficits of the LR1 solution and, thus, achieves significantly higher dynamics. The dynamics is evaluated analogue to Section 5.2 by means of nominal and disturbance steps of ± 500 N in the Z direction. Due to the path planning by the CNC, the force set point does not change abruptly, but follows a 7-segment profile, for which speed, acceleration, and jerk limit values of the force change are chosen very high for this experiment. As a result, the force controller follows the nominal jumps very well with an overshoot of 2.2% (to 1000 N) or 5% (to 500 N), respectively. The disturbance jumps settle after an overshoot of 24.5% within 160 ms (entering the 5% tolerance band) [5]. In comparison, solution LR1 shows up to 99% overshoot and a settling time of 260 ms for the disturbance jumps. Finally, for the LR2 solution, the delay time for the actuating value connection is also evaluated by a step change of 1 mm in the manipulated value: After a dead time of only one control cycle of $T_{d1} = 2$ ms, the set point is passed to the position controller, and after a dead time of $T_d = 12$ ms a change of the actual value is detected. Taking into account a measuring time of 2 ms, the actual value is present at the encoder after 10 ms. This results in a significantly better response behaviour compared to solution LR1 with $T_d = 22$ ms.

The further validation is based on different contour tracking tasks in constant and variable task coordinate systems. In contrast to the flat steel sheet used as workpiece in Section 5.2, contours with significant deviations in the centimetre range from the programmed contour are now used, which the force controller must be able to handle as disturbances. The tools are also slightly redesigned, but follow the same principle of rolling motion on the workpiece with adjustment of contact compliance by means of different springs.

Listing 2: G-Code for contour following by hybrid force/position control [82]

```
N00 #TRAFO OFF ; Deactivate kinematic trafo
N05 #KIN ID[65] ; Select Euler angles
N10 V.G.KIN_STEP[0].ID[65].PARAM[15] = -1 ; -Z force dir.
N15 [...] ; Further parameters
N20 #TRAFO ON ; Activate kinematic trafo
N25 G90 G93 ; Abs. coord., inv. time feed
N30 G0 X=-230 Y=120 Z=-245 U=0 V=0 W=0 ; Goto start pos.
N35 M72 ; Tare force sensor
N40 M52 M51 ; Search contact
N45 G60 ZF=250 F5 ; Control set force
N50 M53 ; Select hard parameters
N55 G1 X=+230 ZF=250 F155 ; Hybrid force/position control
N60 M50 ; Stop force control
N65 M30 ; End
```

Listing 3: Hybrid and parallel force/position control by feed forward of Z coordinates [82]

```
N55 G1 X=-100 Z=-250 ZF=250 F50 ; Point 1
N56 G1 X=-35 Z=-235 ZF=250 F22 ; Point 2
N57 G1 X=55 Z=-250 ZF=250 F35 ; Point 3
N58 G1 X=175 Z=-195 ZF=250 F44 ; Point 4
N59 G1 X=230 Z=-250 ZF=250 F18 ; Point 5
```

5.3.1. Constant task frame

First, a contour tracking task in a constant task coordinate system is used for the basic functional verification of the LR2 solution approach. For this purpose, a roll (tool) attached to the end-effector is moved with active position control in the X-direction and force control in the Z-direction over a contour (workpiece) initially unknown to the control system, Fig. 11. Accordingly, the natural boundary conditions $\mathbf{0} = (f_x, f_y, v_z)^T$ and the artificial boundary conditions $\{x, y, f_z\}$ with a selection matrix Ξ apply to the relevant translatory motions for all degrees of freedom to $\Xi_{diag} = (0 \ 0 \ 1 \ 0 \ 0 \ 0)^T$.

The motion specification is now done by G-Code as shown in Listing 2: After selecting the kinematic transformation and parametrizing the selection matrix, the transformation is activated and the start position is approached (N05-N30). Subsequently, the taring of the force measurement systems, the contact search with soft parameters, the adjustment of the target force at the start position and switching to harder controller parameters (N35-N50) is performed. In the first test without contour pre-control, a programmed movement from $X = -230$ mm to $X = 230$ mm takes place with a constant force of $ZF = 250$ N (N55), after which the force control and the NC programme are terminated (N60-N65). In a second experiment, Listing 3, the Z contour is made known to the control system by five roughly measured reference points using a ruler, and hybrid/parallel force/position control is implemented with this feed-forward control of the Z coordinate. The travel times are divided according to the segment length to ensure a comparable speed and total travel time (N55-N59).

Fig. 12 shows the results for both experiments: without feed-forward (left) and with feed-forward (right). The upper plots show the outputs of CNC and force controller in the Z-direction and the resulting actual positions along the workpiece length in the X-direction. The addition of the CNC (green) and force controller (red) components results in the actual contour of the component in each case, as is clearly visible for both experiments (blue). Here, the disturbance that has to be compensated by the force controller after the addition of the feed-forward contour in the NC programme is significantly smaller at approx. 16.5 mm (right) than in the case without feed-forward, in which it is approx. 56.6 mm (left). Accordingly, the actual forces can be kept at the constant target force and the disturbances can be compensated with maximum deviations of 2.7% (with feedforward) and 5.9% (without feedforward), as shown in the diagrams below. As

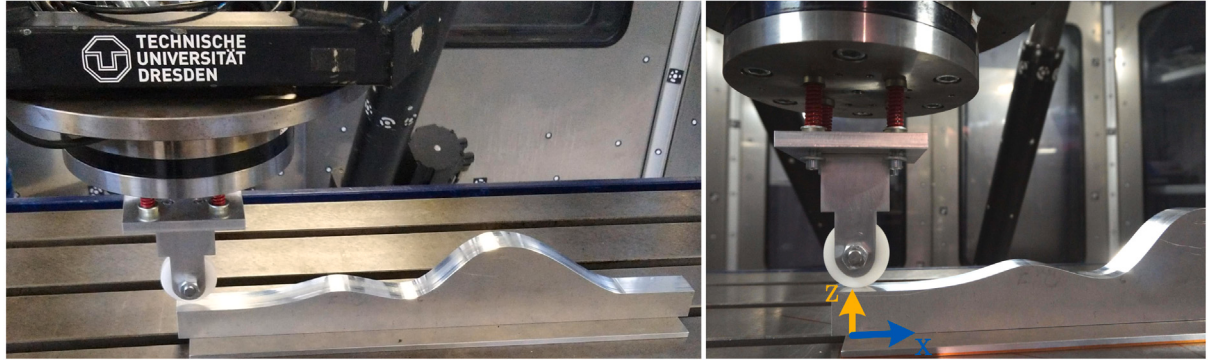


Fig. 11. Validation of motion-synchronous force control LR2 by contour following with constant coordinates (position control in X, force control in Z) [5,82].

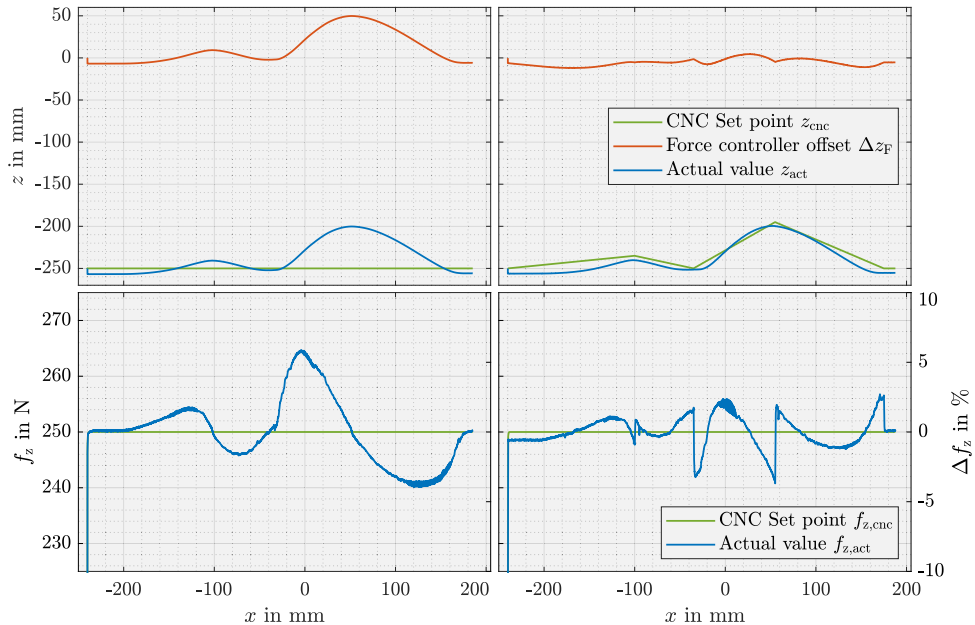


Fig. 12. Results of contour following experiment using hybrid/parallel force control and structure-integrated force sensors in the end-effector platform (1b); top: positions in Z-direction from CNC and force controller as well as resulting actual position; below: nominal and actual forces; left: without feed forward in Z, right: with feedforward of the contour by 5 points; [5,82].

expected, the largest force deviations occur at the points of the largest slope of the contour.

Although the feed rate in the X-direction is significantly lower compared to the feed rate of the LR1 solution in Section 5.2, a significantly higher feed rate of the force control in the Z-direction is achieved due to the significant disturbance contour. Here, this is 2.9 mm/s (without feed-forward) and 1.6 mm/s (with feed-forward) compared to the feed-forward of 0.1 mm/s of the experiment for solution LR1 in Section 5.2 and thus indicates a higher dynamic of solution LR2. The significant disturbance contour also results in high lateral forces on the tool in the X-direction, which may not be desirable. In addition to adjusting the feed rate of the CNC movement, normal force control is a possible solution. This requires a variable task coordinate system and is presented in the following.

5.3.2. Variable task frame

For some use cases, the definition of the task coordinate system is not constant. Typical examples are the rotation of a crank in handling technology or the process force control normal to the workpiece surface in production engineering [41]. To validate the LR2 solution for these applications, two test workpieces with circular and kidney-shaped contours, respectively, are used, as shown in Fig. 13.

For this case, the position control is performed in X-Y coordinates and the force control radially in the direction of a previously defined circle centre $\{x_0, y_0\}$ or normal to the workpiece surface. In addition to the constant CNC coordinate system, the task definition in the task coordinate system also remains constant with the help of the artificial boundary conditions $\{f_n, t, b\}$ and the selection matrix $\Xi_{diag} = (1 \ 0 \ 0 \ 0 \ 0 \ 0)^T$. Only the definition of the task coordinate system relative to the CNC coordinate system is position-dependent. In the selected example, the rotation around the Z-axis with the angle γ is performed by

$$T_F = T(\mathbf{x}, R_z(\gamma)) T_{NC}, \text{ with} \quad (27)$$

$$\gamma = \begin{cases} \text{atan2}\left(\frac{y_0 - y}{x_0 - x}\right) & \text{for radial force control} \\ \text{atan2}\left(\frac{f_y}{f_x}\right) & \text{for normal force control.} \end{cases} \quad (28)$$

Control in the ‘radial’ direction is based purely on geometric variables, whereas control in the normal direction uses measured forces to determine the direction and can therefore only be activated when the measured force values are sufficiently stable [82]. For validation, three experiments are carried out: the radial force control on the circular and the kidney-shaped test piece as well as the normal force control on the kidney-shaped test piece. As described in Section 4.3, the extended

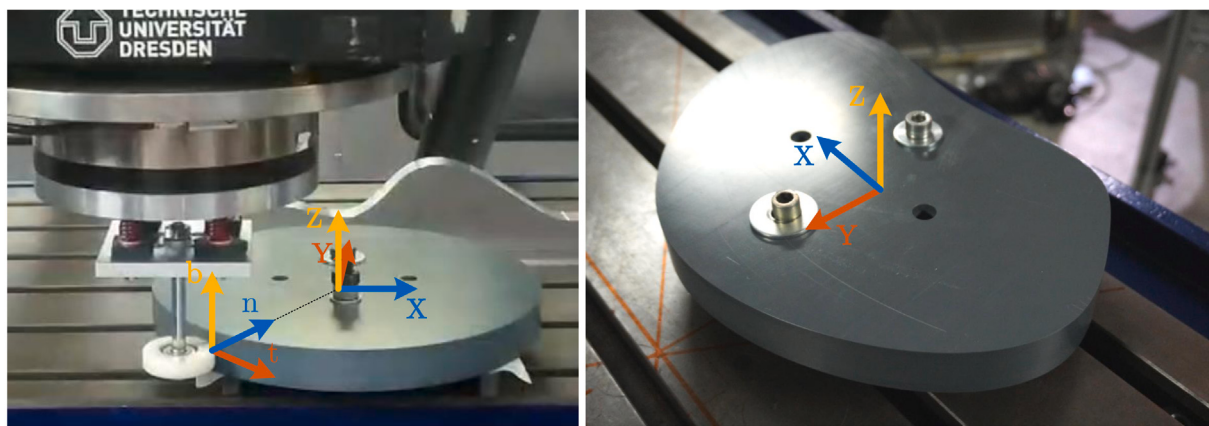


Fig. 13. Validation of force control by contour following with variable coordinates; left: circular test piece, right: kidney-shaped test piece (position control in X and Y direction, force control in radial or normal direction, resp.) [5,82].

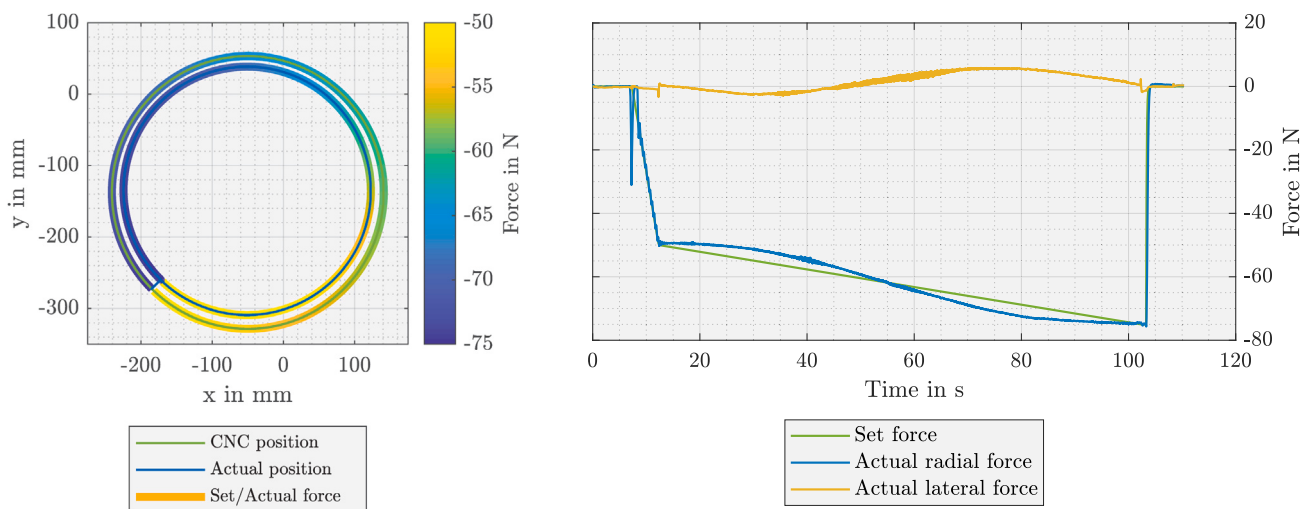


Fig. 14. Contour following results for the circular test piece with variable task coordinates and radial force control using the structure-integrated force sensors in the end-effector platform (1b) [5,82].

functions are also available via parameters and M commands in the G-Code. Listing 4 shows the NC programme for the experiments with the known procedure: Parametrization according to the use case, activation of the kinematic transformation, approaching the start position and taring the force sensors (N00-N40). Subsequently, the variable taskspace is activated, which always starts in the ‘radial force control’ mode, and the contact search is carried out in the direction of the programmed centre point (N45-N50). Only when the contact force is sufficiently large, the normal force control can be activated (N55). After reaching the nominal force at the starting point, the contact force control is carried out during the movement along the programmed circular path in the radial or normal direction, respectively, and, in the end, force control and NC programme are finished (N60-N75). [82]

The results of contour tracking of the circular test piece with radial force control are shown in Fig. 14. Starting from the programmed outer nominal circular path, the force controller corrects successfully the position in the direction of the centre point, so that contact with the workpiece is maintained and the real contour is followed, as can be seen from the nominal and actual forces along the nominal and actual contours on the left. At the same time, the actual force is controlled correctly to the nominal force, which is interpolated along the contour, with deviations of max. 6.5%, as shown on the right. Since the force control in direction of the specified centre point is not normal to the workpiece surface, also lateral forces are generated, which may not be

Listing 4: G-Code for hybrid/parallel radial and normal force control with variable task coordinate system [82]

```

N00 #TRAFO OFF          ; Deactivate kinematic trafo
N05 #KIN ID[65]          ; Select Euler angles
N10 [...] ID[65].PARAM[11] = 1 ; Radial force control
N15 [...] ID[65].PARAM[43] = -50 ; Mid point X
N20 [...] ID[65].PARAM[44] = -137.5 ; Mid point Y
N25 #TRAFO ON            ; Activate kinematic trafo
N30 G90 G161 G93         ; Abs. coord., inv. time feed
N35 G0 X=-165 Y=252.5 Z=-270 U=0 V=0 W=0 ; Goto start
N40 M72                  ; Tare force sensor
N45 M55                  ; Variable task space (radial ctrl)
N50 M51                  ; Search contact
N55 M57                  ; OPTIONAL: Set normal force ctrl
N60 G1 XF=-50 F5          ; Control set force
N65 G3 X=-165 I=-50 J=-137.5 XF=-75 F90
; Circular path with force ctrl and force feed forward
N70 M50                  ; Deactivate force control
N75 M30                  ; End

```

desired. These lateral forces increase with contour derivation from the circular shape as well as the centre offset. [82].

Accordingly, this is particularly important for radial force control on the kidney-shaped test piece, where the lateral forces of up to 60 N even exceed the nominal forces in some cases. The solution is to control

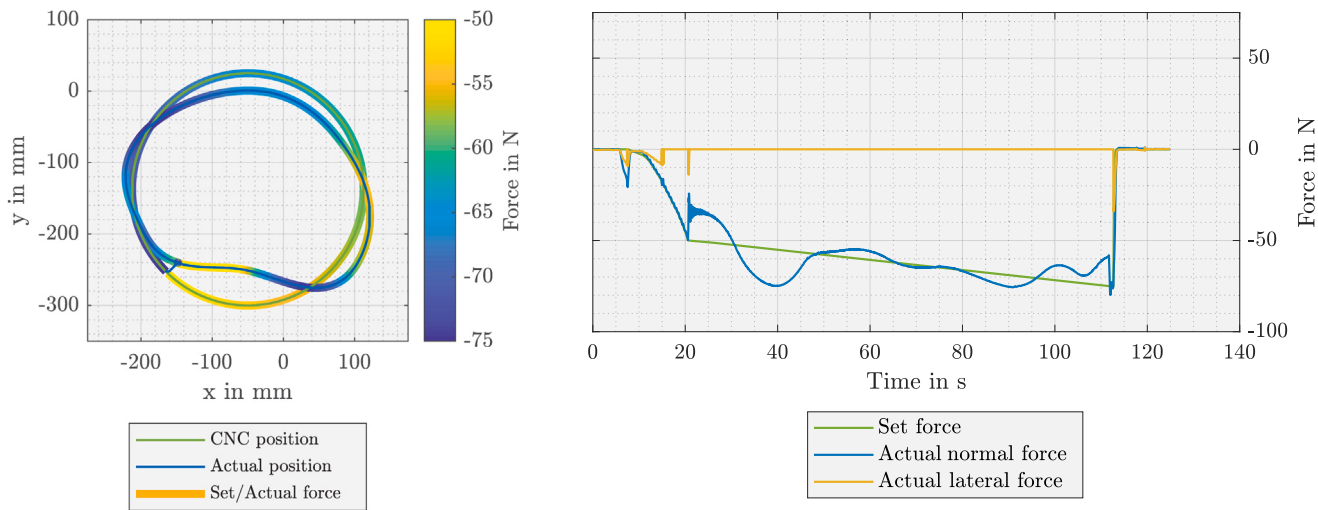


Fig. 15. Contour following results of the kidney-shaped test piece with normal force control using the structure-integrated force sensors in the end-effector platform (1b) [5,82].

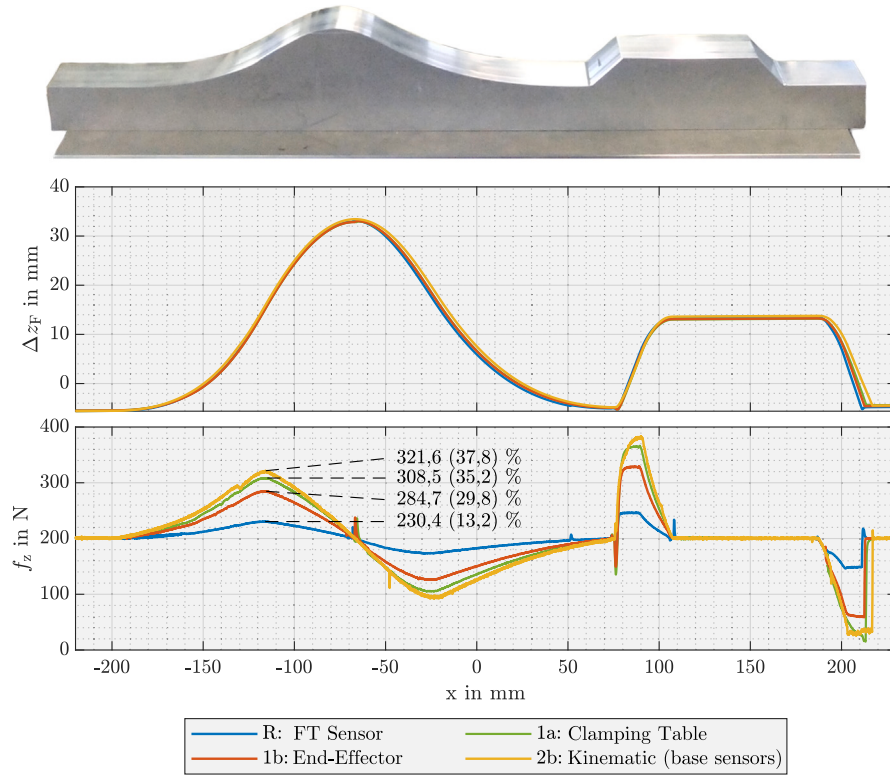


Fig. 16. Comparison of the structure-integrated force measuring systems with regard to their suitability for the force control by contour tracking of a sample workpiece; top: sample workpiece, centre: force controller offset, below: actual force values at a force set point of 200 N [5].

in the normal direction on the basis of the measured forces, Eq. (28), which can be achieved with M57 after sufficiently large contact forces have been built up. As a result, the lateral forces remain close to zero, Fig. 15.

5.4. Influence of the structure-integrated force sensors

Finally, the performance of the structure-integrated force measurement systems regarding force control shall be compared to the reference force measurement platform. To do so, for all force measurement

systems in the hexapod FELIX I the parameters of the force controllers are experimentally determined using the ZIEGLER–NICHOLS rules for a Z force of 200 N, finding the parameters as presented in Table 3. With increasing distance of the measuring systems to the TCP, the stability limit decreases and the controllers have to be parametrized softer. This corresponds to the expectations resulting from the investigation of the dynamic behaviour in [2,3,36]. Higher force filter times allow to increase the controller gain K_p , but have only a minor influence on the achievable reset time T_n .

Table 3

Experimentally found controller parameters for structure-integrated force measuring systems during contact in Z direction; K_p in $\mu\text{m}/\text{N}$, T_n in ms.

Sensor system	$T_l = 50 \text{ ms}$		$T_l = 100 \text{ ms}$		$T_l = 200 \text{ ms}$	
	K_p	T_n	K_p	T_n	K_p	T_n
R FT Sensor	10	7	15	5	40	5
1a Clamping Table	8	10	8	14	26	10
1b End-Effectuator	5	12	8	12	15	12
2b Kinematic	1,5	20	2	20	2	16

Subsequently, with these settings, an additional force-controlled contour tracking in Z-direction is carried out with a second contour that now also contains discontinuities, Fig. 16 above. With a nominal force of 200 N, a filter time of $T_l = 100 \text{ ms}$, and a feed rate of approx. 56 mm/min, the actual force curves shown in Fig. 16 below result. For the force measurement systems, the individual controller parameters result in different dynamics with control deviations of different magnitudes, which are shown in the graph as an example for the first slope. While there is a control deviation of 13.2% for the force measurement platform (R), the integrated force measurement systems show deviations between 29.8% (1b) and 37.8% (2b). The control deviations correlate with the rise of the contour, so that despite the smaller total height, the deviations for the second, unsteady rise are correspondingly greater. With up to 34 mm stroke, the offset to be realized by the force controller is significantly larger than necessary for many applications, such as grinding.

In summary, all the force measurement systems examined are basically suitable for force control. For many applications, the lower dynamics of the structure-integrated measuring systems can be taken into account by correspondingly lower feed rates, so that the maximum control deviations required by the application are fulfilled. For applications that require very high dynamics, force measurement systems close to the TCP are to be preferred.

6. Conclusion

Based on a new approach of structure-integrated force measurement in hexapod machine tools, options to realize force control with the integrated sensors and a commercial numeric control have been studied. As a result of the work, the structure integrated force measuring systems are suitable for force control and the infrastructure of commercial control software can be used to satisfy the needs of force control. Several variants for the realization of a spatial force control are available, which meet the practical application cases defined at the beginning: The LR1 variant with external set point specification by various interfaces, PLC-integrated path planning, and a user interface is particularly suitable for teach-in. The LR2 variant with G-Code integration represents a practical solution for programming force controlled machine tools with easy and concise process control from the NC programme. The CNC interpolates force and position set points synchronously, and, further, can be used to monitor actual force values. By dispensing with integrated path planning and the clock-synchronous integration into the CNC task, the LR2 solution also achieves higher controller dynamics. Variable task frames are programmable and allow realization of a variety of practical relevant applications.

For the structure-integrated force sensor technology, the suitability for force control can be demonstrated. There are advantages in particular for teach-in, which also allows teaching on the machine structure due to the structure integration and greater distance from the TCP, and thus gains significantly in comfort and safety. In contact force control, the structure-integrated measuring systems achieve a little lower dynamics, when compared to FT sensors, which must be taken into account by adjusting the feed rate in order to maintain the permissible control deviation. In future works, more advanced force control methods should be studied using structure-integrated force sensors to further improve the control performance.

Abbreviations and symbols

The following abbreviations and symbols are used in this manuscript:

${}^A(\cdot)_B$	Coordinate vector/tensor: top left reference frame, bottom right body frame
(\cdot)	Spatial vector (6×1)
$(\cdot)^{-T}$	Transposed inverse
$S(\cdot)$	Cross product matrix
$\{T\}, \{P\}, \{B\}$	Table, Platform, and Base frame
$(\cdot)_{\text{nom}}, (\cdot)_{\text{act}}$	Nominal and actual values
$(\cdot)_{\text{cnc}}$	CNC output
$(\cdot)_{\text{cmd}}$	Commanded values for drive controllers
f_q, f_{q0}, f_K, f_q^*	Measured forces, sensor bias, correction values, and processed sensor forces
$\underline{f}_{\text{Ext}}, \underline{f}_{\text{Dyn}}, \underline{f}_G$	External, Dynamic, and Gravitational spatial forces and moments
$J_P, J_{\text{Hex}}(\underline{x})$	Jacobian of sensor framework and hexapod kinematic, A: analytic, G: geometric
$m_p, {}^P x_C, {}^P I_p$	Platform mass, centre of gravity, and inertia
q, \dot{q}, \ddot{q}	Position, velocity, acceleration of the drives
$x, {}^B o_p, {}^B R_p$	Pose, position, and orientation of the TCP
$v, {}^B \dot{o}_p, {}^B \omega_p$	Velocity, translational velocity, and angular velocity of the TCP
$\ddot{v}, {}^B \ddot{o}_p, {}^B \dot{\omega}_p$	Acceleration, translational acceleration, and angular acceleration of the TCP
M_p, C_p, g_p	Mass matrix, matrix of centrifugal and Coriolis terms, gravitational terms
${}^A X_B, {}^A X_B^F$	Spatial motion and force transformation
Ξ	Selection matrix
K_{Fx}, K_{Fq}	Force controller in Cartesian and joint space
$\Delta x_F, \Delta q_F$	Pose and joint offsets due to force control
K_p, T_N, T_V, T_l	PID-Controller parameters
s	LAPLACE parameter
CNC	Computerized Numerical Control
DoF	Degree of Freedom
FK	Forward Kinematic transformation
IPO	Interpolator
IK	Inverse Kinematic transformation
LR1, LR2	Force Control Solution approaches
PLC	Programmable Logic Controller
TCP	Tool Centre Point
UC1, UC2, UC3	Use Cases of force control

CRedit authorship contribution statement

C. Friedrich: Conceptualization, Methodology, Software, Validation, Formal analysis, Investigation, Data curation, Writing – original draft, Writing – review & editing, Visualization, Project administration, Funding acquisition. **F. Schlüter:** Software, Validation, Formal analysis, Data curation, Writing – original draft. **S. Ihlenfeldt:** Resources, Supervision, Project administration, Funding acquisition.

Declaration of competing interest

The authors declare the following financial interests/personal relationships which may be considered as potential competing interests: Christian Friedrich reports financial support was provided by German Research Foundation (DFG).

Data availability

Data will be made available on request.

Acknowledgements

The authors are grateful to the German Research Foundation (DFG) who supported this work with the projects “Fundamentals for structure-integrated measurement and control-integrated processing of spatial forces and torques in machine tools” (DFG No 202081830). Further the authors want to thank the editors and reviewers for their helpful comments and constructive suggestions with regard to the revision of the paper.

References

- [1] Friedrich C, Kauschinger B, Ihlenfeldt S. Decentralized structure-integrated spatial force measurement in machine tools. *Mechatronics* 2016;40:17–27. <http://dx.doi.org/10.1016/j.mechatronics.2016.08.008>.
- [2] Friedrich C, Kauschinger B, Ihlenfeldt S. Spatial force measurement using a rigid hexapod-based end-effector with structure-integrated force sensors in a hexapod machine tool. *Measurement* 2019;145C:350–60. <http://dx.doi.org/10.1016/j.measurement.2019.05.044>.
- [3] Friedrich C, Kauschinger B, Ihlenfeldt S. Stiffness evaluation of a hexapod machine tool with integrated force sensors. *J Mach Eng* 2020;20(1):58–69. <http://dx.doi.org/10.36897/jme/117786>.
- [4] Friedrich C, Ihlenfeldt S. Model calibration for a rigid hexapod-based end-effector with integrated force sensors. *MDPI Sens* 2021;21(10):3537. <http://dx.doi.org/10.3390/s21103537>.
- [5] Friedrich C. Räumliche Kraftmessung und -regelung mit Parallelkinematiken unter Verwendung strukturintegrierter Kraftsensorik (Ph.D. thesis), Technische Universität Dresden; 2022, <https://nbn-resolving.org/urn:nbn:de:bsz:14-qucosa2-827704>.
- [6] Stefanescu DM. *Handbook of force transducers: principles and components*. Springer; 2011.
- [7] Hesselbach J, Behrens B-A, Dietrich F, Poelmeyer J, Rathmann S. Regelungskonzept für eine umformmaschine auf basis einer parallelstruktur und simulative ermittlung von prozessgerechten maschinenparametern. In: *Fertigungsmaschinen mit parallelkinematiken*. Shaker Verlag Düren; 2008, p. 307–22.
- [8] Tönshoff H, Denkena B, Heimann B, Holz C, Abdellatif H. Modellgestützte steuerung und kraftregelung von parallelkinematiken. In: *Fertigungsmaschinen mit Parallelkinematiken*. Shaker Verlag; 2008, p. 323–47.
- [9] Altintas Y, Park S. Dynamic compensation of spindle-integrated force sensors. *CIRP Ann Manuf Technol* 2004;53(1):305–8.
- [10] Byrne G, O'Donnell G. An integrated force sensor solution for process monitoring of drilling operations. *CIRP Ann Manuf Technol* 2007;56(1):89–92.
- [11] Jun MB, Ozdoganlar OB, DeVor RE, Kapoor SG, Kirchheim A, Schaffner G. Evaluation of a spindle-based force sensor for monitoring and fault diagnosis of machining operations. *Int J Mach Tools Manuf* 2002;42(6):741–51.
- [12] Denkena B, Brinkhaus J, Lange D. Possibilities of sensor transponders in machine tools. In: 10th international scientific conference on production engineering, computer integrated manufacturing and high speed machining. 2005, p. 11–3.
- [13] Litwinski K. Sensorisches spannsystem zur Überwachung von Zerspanprozessen in der Einzelteilelfertigung (Ph.D. thesis), Universität Hannover; 2011.
- [14] Denkena B, Kiesner J. Strain gauge based sensing hydraulic fixtures. *Mechatronics* 2016;34:111–8.
- [15] Boudaoud M, Regnier S. An overview on gripping force measurement at the micro and nano-scales using two-fingered microrobotic systems. *Int J Adv Robot Syst* 2014;11.
- [16] Denkena B, Litwinski K, Brouwer D, Boujnah H. Design and analysis of a prototypical sensory Z-slide for machine tools. *Prod Eng* 2013;7(1):9–14.
- [17] Denkena B, Dahlmann D, Boujnah H. Sensory workpieces for process monitoring - an approach. *Proc Technol* 2016;26:129–35.
- [18] Loughlin C, Albu-Schäffer A, Haddadin S, Ott C, Stemmer A, Wimböck T, Hirzinger G. The DLR lightweight robot: design and control concepts for robots in human environments. *Ind Robot: Int J* 2007;34(5):376–85.
- [19] Ott C, Roa MA, Schmidt F, Friedl W, Englsberger J, Burger R, Werner A, Dietrich A, Leidner D, Henze B, et al. Mechanisms and design of DLR humanoid robots. In: Goswami A, Vadakkepat P, editors. *Humanoid robotics: a reference*. Springer Dordrecht; 2016, p. 1–26.
- [20] Grotjahn M, Daemi M, Heumann B. Friction and rigid body identification of robot dynamics. *Int J Solids Struct* 2001;38(10):1889–902.
- [21] Jubien A, Gautier M, Janot A. Dynamic identification of the kuka LWR robot using motor torques and joint torque sensors data. *IFAC Proc Vol* 2014;47(3):8391–6.
- [22] Sorli M, Pastorelli S. Six-axis reticulated structure force/torque sensor with adaptable performances. *Mechatronics* 1995;5(6):585–601.
- [23] Li F. Design and analysis of a fingertip stewart platform force/torque sensor (Ph.D. thesis), Simon Fraser University; 1998.
- [24] Aghili F, Buehler M, Hollerbach JM. Design of a hollow hexaform torque sensor for robot joints. *Int J Robot Res* 2001;20:967–76.
- [25] Kang C-G. Closed-form force sensing of a 6-axis force transducer based on the Stewart platform. *Sensors Actuators A* 2001;90(1):31–7.
- [26] Dwarakanath T, Bhutani G. Beam type hexapod structure based six component force/torque sensor. *Mechatronics* 2011;21(8):1279–87.
- [27] Röske D. Multi-component measurements of the mechanical quantities force and moment. In: Fachorgan für Wirtschaft und Wissenschaft Amts- und Mitteilungsblatt der physikalisch-technischen Bundesanstalt Braunschweig und Berlin. 118,2,3, 2008, p. 56–9.
- [28] Nitsche J, Baumgarten S, Petz M, Röske D, Kumme R, Tutsch R. Measurement uncertainty evaluation of a hexapod-structured calibration device for multi-component force and moment sensors. *Metrologia* 2017;54(2):171.
- [29] Genta G, Germak A, Barbato G, Levi R. Metrological characterization of an hexapod-shaped multicomponent force transducer. *Measurement* 2016;78:202–6.
- [30] Genta G, Prato A, Mazzoleni F, Germak A, Galetto M. Accurate force and moment measurement in spring testing machines by an integrated hexapod-shaped multicomponent force transducer. *Meas Sci Technol* 2018;29(9):095902.
- [31] Palumbo S, Germak A, Mazzoleni F, Desogus S, Barbato G. Design and metrological evaluation of the new 5 MN hexapod-shaped multicomponent build-up system. *Metrologia* 2016;53(3):956.
- [32] Seibold US. An advanced force feedback tool design for minimally invasive robotic surgery (Ph.D. thesis), Technische Universität München; 2013.
- [33] Matich S, Hessinger M, Kupnik M, Werthschützky R, Hatzfeld C. Miniaturized multiaxial force/torque sensor with a rollable hexapod structure. *Tm-Tech Messen* 2017;84(s1):138–42.
- [34] A.G. OH. Kräfte messen mit hexamove-konzept. *Produktprospekt: Hexamove - Bewegung Leichtgemacht* 2017;16:17.
- [35] Wang Y, Hou S, Zhang R, Tang X. Interaction force measurement of parallel robots based on structure-integrated force sensors using interpretable linear neural networks. *Mechatronics* 2022;87:102895.
- [36] Friedrich C, Ihlenfeldt S. Spatial compliance measurement of a clamping table with integrated force sensors. *J Mach Eng* 2022;22(1). <http://dx.doi.org/10.36897/jme/146533>.
- [37] Whitney DE. Historical perspective and state of the art in robot force control. *Int J Robot Res* 1987;6(1):3–14.
- [38] Patarinski SP, Botev RG. Robot force control: a review. *Mechatronics* 1993;3(4):377–98.
- [39] Yoshikawa T. Force control of robot manipulators. In: *Robotics and automation, 2000. Proceedings. ICRA'00. IEEE international conference on*, Vol. 1. IEEE; 2000, p. 220–6.
- [40] Canudas de Wit C, Siciliano B, Bastin G, editors. *Theory of robot control*. Springer London; 1996.
- [41] Siciliano B, Khatib O, editors. *Handbook of Robotics*. Springer-Verlag Berlin Heidelberg; 2016.
- [42] Siciliano B, Sciacivico L, Villani L, Oriolo G. *Robotics*. Springer London; 2010.
- [43] Spong MW, Hutchinson S, Vidyasagar M. *Robot modeling and control*, Vol. 3. NY: Wiley; 2006.
- [44] Siciliano B, Villani L. *Robot force control*. Springer Science + Business Media; 1999.
- [45] Salisbury JK. Active stiffness control of a manipulator in cartesian coordinates. In: *Decision and control including the symposium on adaptive processes, 1980 19th IEEE conference on*. IEEE; 1980, p. 95–100.
- [46] Hogan N. Impedance control-an approach to manipulation. I-Theory. II-implementation. III-applications. *ASME Trans J Dyn Syst Meas Control* B 1985;107:1–24.
- [47] Fazio TL, Selter DS, Whitney DE. The instrumented remote center of compliance. *Ind Robot* 1984;11:238–42.
- [48] Spong MW. On the force control problem for flexible joint manipulators. *IEEE Trans Automat Control* 1989;34(1):107–11.
- [49] Sciacivico L, Siciliano B. *Modelling and control of robot manipulators (advanced textbooks in control and signal processing)*. Springer; 2000.
- [50] Chiaverini S, Sciacivico L. The parallel approach to force/position control of robotic manipulators. *IEEE Trans Robot Autom* 1993;9(4):361–73.
- [51] Chiaverini S, Siciliano B, Villani L. Force/position regulation of compliant robot manipulators. *IEEE Trans Automat Control* 1994;39(3):647–52.
- [52] De Schutter J, Van Brussel H. Compliant robot motion II. A control approach based on external control loops. *Int J Robot Res* 1988;7(4):18–33.
- [53] Mason MT. Compliance and force control for computer controlled manipulators. *IEEE Trans Syst Man Cybern* 1981;11(6):418–32.
- [54] Raibert MH, Craig JJ. Hybrid position/force control of manipulators. *J Dyn Syst Meas Control* 1981;103(2):126–33.
- [55] Bruyninxkx H, De Schutter J. Specification of force-controlled actions in the “task frame formalism” - a synthesis. *IEEE Trans Robot Autom* 1996;12(4):581–9.
- [56] Spiller A. *Unterstützung der Werkstückhandhabung kooperierender Industrieroboter durch Kraftregelung* (Ph.D. thesis), Universität Stuttgart; 2014.
- [57] Zivanovic MD, Vukobratovic M. Multi-arm cooperating robots: dynamics and control, Vol. 30. Springer Science & Business Media; 2006.
- [58] Magrini E, Flacco F, De Luca A. Control of generalized contact motion and force in physical human-robot interaction. In: *Robotics and automation (ICRA), 2015 IEEE international conference on*. IEEE; 2015, p. 2298–304.

- [59] Großmann K, Mühl A. Adaptiv geregeltes Fräsen auf einem Hexapoden. Schriftenreihe des Lehrstuhls für Werkzeugmaschinen; 2004.
- [60] Becker O. Kraftregelungsverfahren für hydraulisch angetriebene nichtkartesische Fertigungsmaschinen (Ph.D. thesis), TU Braunschweig; 2003.
- [61] Hesselbach J, Rathmann S. Hexapoden für die flexible umformung. Werkstatttech Online 2005;793–7.
- [62] Hesselbach J, Behrens B-A, Dietrich F, Rathmann S, Poelmeyer J. Flexible forming with hexapods. Prod Eng 2007;1(4):429–36.
- [63] Grotjahn M. Kompensation nichlinearer dynamischer Effekte bei seriellen und parallelen Robotern zur erhöhung der Bahngenaugkeit (Ph.D. thesis), Universität Hannover; 2003.
- [64] Grendel H. Entwurf und Regelung einer parallelkinematischen Maschine mit hoher Dynamik (Ph.D. thesis), Universität Hannover; 2004.
- [65] Abdellatif H. Modellierung, Identifikation und robuste Regelung von Robotern mit parallelkinematischen Strukturen (Ph.D. thesis), Universität Hannover; 2007.
- [66] Holz C. Positions- und Kraftregelung eines linear direkt angetriebenen Hexapoden (Ph.D. thesis), PZH, Produktionstechn. Zentrum; 2007.
- [67] Raatz C, Rehn S, Petrak A, Großmann K, Wagenführ A. Thermoglättungen von holzwerkstoffen mittels parallelkinematischer bewegungseinheit. Holztechnologie 2009;50:17–22.
- [68] Reisinger T. Kontaktregelung von Parallelrobotern auf der Basis von Aktionsprimitiven (Ph.D. thesis), TU Braunschweig; 2008.
- [69] Reisinger T, Wobbe F, Kolbus M, Schumacher W. Integrated force and motion control of parallel robots-part 2: Constrained space. In: Robotic systems for handling and assembly. Springer; 2010, p. 253–73.
- [70] Kolbus M, Wobbe F, Reisinger T, Schumacher W. Integrated force and motion control of parallel robots-part 1: Unconstrained space. In: Robotic Systems for Handling and Assembly. Springer; 2010, p. 233–52.
- [71] Kohlstedt A, Olma S, Flottmeier S, Traphöner P, Jäker K-P, Trächtler A. Control of a hydraulic hexapod for a hardware-in-the-loop axle test rig. At-Automatisierungstechnik 2016;64(5):365–74.
- [72] Kozlowski D, Stoughton R, Newman W, Hebbal R. Automated force controlled assembly utilizing a novel hexapod robotic manipulator. In: Automation Congress, 2002 Proceedings of the 5th Biannual World. 14, IEEE; 2002, p. 547–52.
- [73] Le Flohic J, Paccot F, Bouton N, Chanal H. Application of hybrid force/position control on parallel machine for mechanical test. Mechatronics 2018;49:168–76.
- [74] Bellakehal S, Andreff N, Mezouar Y, Tadjine M. Commande vision/force de robots parallèles. J Eur Syst Autom 2010.
- [75] Lindenroth L, Stoyanov D, Rhode K, Liu H. Toward intrinsic force sensing and control in parallel soft robots. IEEE/ASME Trans Mechatronics 2022.
- [76] Featherstone R. Rigid body dynamics algorithms. Springer Nature; 2008.
- [77] Friedrich C, Großmann K. Strukturintegrierte kraftmessung. Teil 3 - wirkstellenferne messung. ZWF 2016;1–2:36–40. <http://dx.doi.org/10.3139/104.111396>.
- [78] Vogt R. Entwicklung und Umsetzung einer Kraftregelung mit strukturintegrierter Kraftsensorik an einem Hexapod (Master's thesis), TU Dresden; 2017.
- [79] Taghirad HD. Parallel robots: mechanics and control. CRC Press; 2013.
- [80] Wiese T. Externe sollwertaufschaltung für eine CNC-steuerung. Studienarbeit 2017;TU Dresden.
- [81] Thiem X, Kauschinger B, Ihlenfeldt S. Online correction of thermal errors based on a structure model. Int J Mech Manuf Syst 2019;12(1):49–62.
- [82] Schlüter F. Räumliche Kraftregelung an einem Hexapod auf Basis strukturintegrierter Kraftsensorik (Master's thesis), TU Dresden; 2021.
- [83] Wiese T. Untersuchungen zur Kraftmessung und -regelung mit strukturintegrierter Sensorik an einem Hexapod (Master's thesis), TU Dresden; 2017.



Dr.-Ing. Christian Friedrich was born in Werdau, Germany in 1984. He received his diploma degree in Mechatronic Engineering from the TU Dresden in 2008 and his Ph.D. degree in 2022. From 2009 to 2021 he was Research Associate with the Institute of Mechatronic Engineering at the Chair of Machine Tools and Adaptive Controls at the TU Dresden. Since 2021 he is Group Leader for Control of Cognitive Production Systems at the Fraunhofer Institute for Machine Tools and Forming Technology. His research interests include robot kinematics, kinetics, and control as well as force measurement and control.



Dipl.-Ing. Frederik Schlüter was born in Troisdorf, Germany in 1995. He received his diploma degree in mechanical engineering from the TU Dresden in 2021. Since 2021 he studies informatics at Ecole 42 in Paris. His research interests include the adaption of classical software architecture principles for industrial informatics and robotics in particular.



Prof. Dr.-Ing. Steffen Ihlenfeldt was born in Aschersleben, Germany in 1971. He received his diploma degree in mechanical engineering from the TU Braunschweig in 1997 and his Ph.D. degree from TU Chemnitz in 2012. From 1997 to 2015 he was Research Associate, Group Leader and Head of Department of Machine Tools and Automation with the Fraunhofer Institute for Machine Tools and Forming Technology (IWT). Since 2015 he is Professor with the Chair of Machine Tools and Adaptive Controls at the TU Dresden and since 2016 Head of Main Department Cyber-Physical-Systems with the Fraunhofer IWT. Since 2021 he is Director with the Fraunhofer IWT.